

Morgana Guilherme de Castro

**Avaliação das técnicas de soldagem Laser, TIG e Plasma de uso odontológico aplicadas às ligas de Co-Cr e Ti-6Al-4V com diferentes configurações de juntas e diferentes diâmetros: análise por meio de teste de tração, teste de flexão, dureza Vicker's, micro-CT e método de elementos finitos**

Tese apresentada ao Programa de Pós-Graduação em Odontologia da Faculdade de Odontologia da Universidade Federal de Uberlândia, para obtenção do Título de Doutora em Odontologia – Área de concentração Clínica Odontológica

Uberlândia  
2016

Morgana Guilherme de Castro

**Avaliação das técnicas de soldagem Laser, TIG e Plasma de uso odontológico aplicadas às ligas de Co-Cr e Ti-6Al-4V com diferentes configurações de juntas e diferentes diâmetros: análise por meio de teste de tração, teste de flexão, dureza Vicker's, micro-CT e método de elementos finitos**

Tese apresentada ao Programa de Pós-Graduação em Odontologia da Faculdade de Odontologia da Universidade Federal de Uberlândia, para obtenção do Título de Doutora em Odontologia – Área de concentração Clínica Odontológica

Orientador: Prof. Dr. Paulo César Simamoto Júnior  
Co-orientador: Prof. Dr. Cleudmar Amaral Araújo

Banca Examinadora:  
Prof. Dr. Paulo César Simamoto Júnior  
Prof. Dr. Cleudmar Amaral Araújo  
Prof. Dr. Alfredo Júlio Fernandes Neto  
Profa. Dra. Germana de Villa Camargos  
Prof. Dr. Luís Henrique Araújo Raposo  
Prof. Dr. Roberto Sales e Pessoa

Uberlândia  
2016

Dados Internacionais de Catalogação na Publicação  
(CIP) Sistema de Bibliotecas da UFU, MG, Brasil.

---

C355a  
2016

Castro, Morgana Guilherme de, 1984

Avaliação das técnicas de soldagem Laser, TIG e Plasma de uso odontológico aplicadas às ligas de Co-Cr e Ti-6Al-4V com diferentes configurações de juntas e diferentes diâmetros: análise por meio de teste de tração, teste de flexão, dureza Vicker's, micro-CT e método de elementos finitos / Morgana Guilherme de Castro. - 2016.

109 f. : il.

Orientador: Paulo César Simamoto Júnior.

Coorientador: Cleudmar Amaral Araújo.

Tese (doutorado) - Universidade Federal de Uberlândia, Programa de Pós-Graduação em Odontologia.

Inclui bibliografia.

1. Odontologia - Teses. 2. Solda e soldagem - Teses. 3. Titânio - Soldagem - Teses. 4. Reabilitação bucal - Teses. I. Simamoto Júnior, Paulo César, 1977. II. Araújo, Cleudmar Amaral. III. Universidade Federal de Uberlândia. Programa de Pós-Graduação em Odontologia. IV. Título.

CDU: 616.314

---



SERVIÇO PÚBLICO FEDERAL  
MINISTÉRIO DA EDUCAÇÃO  
UNIVERSIDADE FEDERAL DE UBERLÂNDIA  
FACULDADE DE ODONTOLOGIA  
PROGRAMA DE PÓS-GRADUAÇÃO EM ODONTOLOGIA



Ata da defesa de TESE DE DOUTORADO junto ao Programa de Pós-graduação em Odontologia da Faculdade de Odontologia da Universidade Federal de Uberlândia.

Defesa de: Tese de Doutorado nº 016 - COPOD

Data: 14/12/2016

Discente: Morgana Guilherme de Castro; Matrícula: (11313ODO009)

Título do Trabalho: Avaliação das técnicas de soldagem Laser, TIG e Plasma de uso odontológico aplicadas às ligas de Co-Cr e Ti-6Al-4V com diferentes configurações de juntas e diferentes diâmetros: análise por meio de teste de tração, teste de flexão, dureza Vicker's, micro-CT e método de elementos finitos.

Área de concentração: Clínica Odontológica Integrada.

Linha de pesquisa: Implantodontia e Prótese sobre Implantes.

Projeto de Pesquisa de vinculação: Implantodontia e Prótese sobre Implantes.

As oito horas do dia **quatorze de dezembro do ano de 2016** no Anfiteatro Bloco 4L Anexo A, sala 23 Campus Umuarama da Universidade Federal de Uberlândia, reuniu-se a Banca Examinadora, designada pelo Colegiado do Programa de Pós-graduação em janeiro de 2016, assim composta: Professores Doutores: Alfredo Júlio Fernandes Neto (UFU); Luis Henrique Araújo Raposo (UFU); Germana de Villa Camargos (UNIFAL); Roberto Sales e Pessoa (UNITRI); Paulo César Simamoto Júnior (UFU) orientador(a) do(a) candidato(a) **Morgana Guilherme de Castro**.

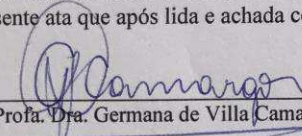
Iniciando os trabalhos o(a) presidente da mesa Dr. Paulo César Simamoto Júnior apresentou a Comissão Examinadora e o candidato(a), agradeceu a presença do público, e concedeu ao Discente a palavra para a exposição do seu trabalho. A duração da apresentação do Discente e o tempo de arguição e resposta foram conforme as normas do Programa.

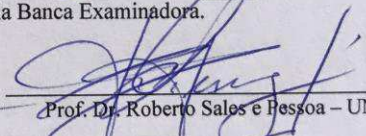
A seguir o senhor(a) presidente concedeu a palavra, pela ordem sucessivamente, aos(às) examinadore(a)(s), que passaram a arguir o(a) candidato(a). Ultimada a arguição, que se desenvolveu dentro dos termos regimentais, a Banca, em sessão secreta, atribuiu os conceitos finais.

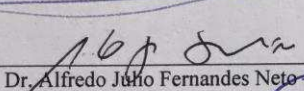
Em face do resultado obtido, a Banca Examinadora considerou o(a) candidato(a) A provado(a).

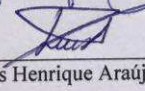
Esta defesa de Tese de Doutorado é parte dos requisitos necessários à obtenção do título de Doutor. O competente diploma será expedido após cumprimento dos demais requisitos, conforme as normas do Programa, a legislação pertinente e a regulamentação interna da UFU.

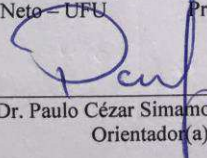
Nada mais havendo a tratar foram encerrados os trabalhos às 13 horas e 30 minutos. Foi lavrada a presente ata que após lida e achada conforme foi assinada pela Banca Examinadora.

  
Prof. Dra. Germana de Villa Camargos – UNIFAL

  
Prof. Dr. Roberto Sales e Pessoa – UNITRI

  
Prof. Dr. Alfredo Júlio Fernandes Neto – UFU

  
Prof. Dr. Luis Henrique Araújo Raposo – UFU

  
Prof. Dr. Paulo César Simamoto Júnior – UFU  
Orientador(a)



## DEDICATÓRIA

A Deus, por ser meu alicerce, Aquele que me faz acreditar que tudo sempre acontece no tempo certo e da melhor forma possível.

A Nossa Senhora de Fátima, Nossa Senhora Aparecida e Nossa Senhora da Abadia. Minha fé e devoção a vocês minhas mãezinhas aí de cima. Sempre intercedendo por mim e me conduzindo aos melhores caminhos.

À minha mãe, Maria de Fátima, por estar sempre presente em todos os momentos da minha vida, me apoiando e incentivando incondicionalmente. Sem você nada seria como é. Você é uma grande inspiração para mim. Amo você infinitamente!

Ao meu Pai, Carlos. Obrigada por todas as oportunidades. Obrigada por me permitir ser a pessoa e a profissional que sou hoje. Amo você.

À minha afilhada, Maria Laura. Com você eu aprendi que o amor é inexplicavelmente grande. Por você eu tento ser, a cada dia, uma pessoa, uma profissional e uma madrinha melhor. Com você a vida é mais leve, mais linda, mais colorida e mais divertida.

Ao meu irmão, Carlos Júnior. Se eu pudesse ter escolhido um irmão, eu com certeza teria escolhido você. Obrigada simplesmente por ser quem você é. Amo você! E à minha cunhada Jesika. Obrigada por me dar o melhor presente da vida, minha afilhada. Obrigada por dividirem este momento comigo.

Aos meus avós, Homero e Sebastiana, que são meu porto seguro e sempre estiveram ao meu lado durante toda minha caminhada nesta vida. Amo muito vocês.

Aos meus tios, Marcel e Silvana, pelos quais tenho uma admiração imensa e muito amor e carinho. Vocês são essenciais na minha vida. Foram essenciais neste momento.

Aos meus primos mais lindos, Leandro, Vítor e Caio. Obrigada pelo carinho,  
amizade e amor.

Ao meu tio Sandro (*in memoriam*), que sei que está aí em cima fazendo festa.  
Você sempre se orgulhou da minha trajetória. Queria que você estivesse aqui  
para dividir este momento comigo.

Ao meu afilhado, Homero Neto. Peço a Deus todos os dias que ele te ilumine e  
te guarde. Que te conduza sempre aos melhores caminhos e te conserve esta  
alma linda. Que de alguma forma eu possa ser um exemplo do bem para você.

À minha prima Sarah, por quem tenho um amor de irmã, que está ao meu lado  
me dando força e me apoiando sempre. E ao seu marido (primo de tabela),  
Douglas, por quem tenho um carinho enorme e sou grata pelo mesmo carinho  
que tem por mim.

À minha sobrinha-prima Cecília. Você veio deixar nossos dias mais cor de rosa  
com certeza. A titia te ama muito e vai estar sempre ao seu lado na caminhada  
da vida.

A vocês dedico este trabalho!

## **AGRADECIMENTOS ESPECIAIS**

Ao Prof. Dr. Paulo Cézar Simamoto Júnior, obrigada por me ensinar uma das lições mais valiosas que aprendi na minha vida profissional: “que tudo é possível, que eu sou capaz”. Obrigada por, muitas vezes, acreditar em mim e em meus ideais, muito mais do que eu mesma. Obrigada por me contagiar com seu entusiasmo. Obrigada por me empurrar sempre para frente. Obrigada por todas as cobranças e todas as oportunidades. Meu orientador de mestrado, doutorado, meu colega de trabalho e meu querido amigo, nosso caminho é longo, temos muito a fazer juntos ainda.

À Profa. Dra. Veridiana Rezende Novais Simamoto. Obrigada pelo carinho, incentivo, paciência e auxílio em todos os momentos. É muito bom poder contar com você. Obrigada por tudo sempre.

Ao Prof. Dr. Cleudmar Amaral Araújo. Obrigada por ser essa pessoa inspiradora. Obrigada por um dia ter me recebido como uma filha no seu laboratório. Obrigada por todas as oportunidades e por toda a importância que você sempre me deu. Tenho por você uma admiração inenarrável e um carinho imenso. Espero que ainda caminhemos juntos por muitos e muitos projetos.

Ao Prof. Dr. Alfredo Júlio Fernandes Neto. Não sei como poderia defender essa tese sem tê-lo comigo neste momento e sem agradecê-lo pela milésima vez. Obrigada por ser este mestre, esta inspiração e este grande ‘paizão’ que é para todos nós. Sempre que me encontrava perdida, você aparecia para me dar bons conselhos. Agradeço por um dia ter acreditado nessa Faculdade e nessa Pós-Graduação, por você hoje podemos nos orgulhar de toda esta construção. Obrigada por ser esta pessoa incomparável com a qual tenho o prazer de conviver.

Ao Prof. Dr. Flávio Domingues das Neves. Obrigada por todas as oportunidades e pelo exemplo que você é pra mim. Sem dúvida, você é responsável por muitas das minhas conquistas profissionais. Te admiro e te respeito muito.

Ao Prof. Dr. Carlos José Soares, por quem tenho um carinho enorme. Obrigada, também, pelas oportunidades e pelo jeito sempre tão gentil e carinhoso que sempre me tratou. Obrigada por tantos, mas tantos conhecimentos adquiridos com você. Obrigada por sempre me ajudar em todas as minhas dificuldades. Seu reconhecimento profissional é fruto deste trabalho grandioso que você faz com muito amor.

À Profa. Sonia Goulart. Obrigada por todo carinho e por todo o conhecimento adquirido com você nas nossas reuniões formais ou informais. Você para mim é sinônimo de mulher forte, de profissional competente e dedicada. Obrigada por tudo.

Ao Prof. Whashington Martins da Silva Júnior, coordenador do Laboratório de Tribologia e Materias da Faculdade de Engenharia Mecânica da Universidade Federal de Uberlândia. Agradeço por me receber com tanto carinho em seu laboratório e por contribuir tanto com as nossas pesquisas. Com certeza essa parceria deu muito certo e vai nos render bons frutos. Obrigada de coração.

Ao Prof. Dr. Ricardo Tadeu Lopes, do Instituto Alberto Luiz Coimbra de Pós-Graduação e Pesquisa de Engenharia, da Universidade Federal do Rio de Janeiro. Agradeço por toda contribuição prestada neste trabalho, por me receber com tanto carinho no Rio de Janeiro e por me permitir acompanhar os trabalhos no maior centro de ensino e pesquisa em engenharia da América Latina. Foi, sem dúvida, uma experiência incrível e edificante.

À Profa. Itzar Minondo do ITMA Materials and Technologies e membro do Comitê Científico do III International Congress & 21st Technical Session on Welding and Joining Technologies. Agradeço por nos convidar a participar deste grandioso evento e levar um dos artigos desta tese para apresentação. Foi, indiscutivelmente, um dos maiores desafios que já tive como pesquisadora, entretanto foi incrivelmente maravilhoso. A única representante da América Latina e única brasileira a participar desse evento. Eu realmente tenho muito a agradecer por essa oportunidade.



Ao meu colega de graduação, colega de trabalho, afilhado de casamento e grande amigo Luís Henrique Araújo Raposo. Tive a certeza, na minha defesa de mestrado, que você realmente era um daqueles amigos que a gente pode contar de verdade. Obrigado por sempre me ajudar, sempre me apoiar e ser sempre tão presente. Ser sua amiga já era bom demais e, ao se casar com a Analice, essa amizade ficou boa em dobro. Aproveito e já agradeço a você minha querida amiga. Caminhamos juntas nesta estrada da pós-graduação e partilhamos muitas histórias, muitas alegrias, muitas angústias e muitas festas. Mas a melhor parte é que nos tornamos grandes amigas e sou eternamente grata por isso.

À minha colega e amiga Profa. Dra. Germana de Villa Camargos. Já são tantas histórias juntas, tantos momentos profissionais e pessoais que dividimos ao longo da vida que poder dividir esse momento com você é um privilégio. Uma profissional super competente, que tem muito a contribuir e uma grande amiga. Obrigada por aceitar o convite para ser banca deste trabalho.

Ao Prof. Dr. Roberto Sales e Pessoa. Agradeço por todas as oportunidades e por todo aprendizado adquirido com você durante todos esses anos. É incrível como qualquer 30 minutos de conversa com você fazem minha mente se abrir para novos conhecimentos. Admiro muito seu trabalho como professor e pesquisador. Agradeço imensamente por ter aceitado o convite para ser banca deste trabalho.

A uma das minhas melhores amigas e minha eterna parceira de pesquisa, Profa. Gabriela Lima Menegaz. Não vivo sem você. Todos os dias agradeço a Deus por ter nos colocado no mesmo caminho. Com você aprendi tanto de engenharia, de generosidade, de doação e de amizade. Nossa parceria vai durar enquanto tivermos fôlego para trabalhar, e nossa amizade... essa vai durar para sempre. Obrigada por existir na minha vida!

## **AGRADECIMENTOS**

À Universidade Federal de Uberlândia (UFU).

À Faculdade de Odontologia da Universidade Federal de Uberlândia (FOUFU).

À Escola Técnica de Saúde da Universidade Federal de Uberlândia (ESTES/UFU).

À Faculdade de Engenharia Mecânica da Universidade Federal de Uberlândia (FEMEC/UFU).

Ao Laboratório de Projetos Mecânicos Prof. Dr. Henner Alberto Gomide (LPM).

Ao Centro de Pesquisa de Biomecânica, Biomateriais e Biologia Celular (CPBio).

Ao Laboratório de Ensino e Pesquisa em Usinagem (LEPU).

Ao Centro para Pesquisa e Desenvolvimento de Processos de Soldagem (LAPROSOLDA).

Ao Laboratório de Tribologia e Materiais.

Aos Laboratórios de Prótese – ESTES-UFU.

Ao Laboratório de Prótese Removível da Faculdade de Odontologia de Piracicaba da Universidade Estadual de Campinas (FOP/UNICAMP).

Ao Instituto Alberto Luiz Coimbra de Pós-Graduação e Pesquisa de Engenharia, da Universidade Federal do Rio de Janeiro (COPPE/UFRJ).

À Coordenação de Aperfeiçoamento de Pessoal de Nível Superior (CAPES).

À Fundação de Amparo à Pesquisa de Minas Gerais (FAPEMIG).

Ao Programa de Pós-graduação em Odontologia da Faculdade de Odontologia da Universidade Federal de Uberlândia (PPG/FOUFU).

Ao Programa de Pós-graduação em Engenharia Mecânica da Faculdade de Engenharia Mecânica da Universidade Federal de Uberlândia (FEMEC/UFU).

Ao Prof. Dr. Américo Scotti. Obrigada pela oportunidade de participar, ainda no mestrado, da disciplina de Soldagem no programa de pós-graduação em engenharia mecânica e por toda ajuda prestada neste trabalho. O reflexo dessa oportunidade está em todos os nossos trabalhos.

Ao Prof. Dr. Henner Alberto Gomide. Obrigada por, desde a época da iniciação científica, estar presente e me ensinar tanto. Tenho um carinho enorme e um respeito ainda maior pelo senhor.

Às professoras e amigas, Dra. Evonete Marra, Dra. Rosana Ono, Ms. Cristiane Pacheco, Ms. Maria Campoli e Dra. Simone Avila, por tantos anos de convivência, carinho e admiração. Jamais vou me esquecer de agradecê-las pelo apoio que sempre encontro em vocês em qualquer época da vida e por todas as oportunidades inenarráveis. Minha gratidão é eterna.

Ao Prof. Dr. Mauro Antônio de Arruda Nóbilo, da Faculdade de Odontologia de Piracicaba da Universidade Estadual de Campinas (UNICAMP) pela contribuição direta a este trabalho.

Ao Prof. Dr. Ricardo Faria Ribeiro, da Faculdade de Odontologia de Ribeirão Preto da Universidade de São Paulo (FORP/USP), por ser um grande exemplo para mim. Não tenho palavras para agradecer sua generosidade em todos os momentos em que precisei da sua ajuda neste e em outros trabalhos. Tenho pelo senhor uma grande admiração e um respeito enorme.

Aos amigos e professores da Faculdade de Odontologia. Obrigada a cada um de vocês por tornarem esta caminhada mais edificante. Vocês são referências valiosas para mim. Em especial, agradeço aos professores Luiz Carlos Gonçalves, Paulo Vinicius Soares, Murilo Menezes, Gisele Rodrigues,

Marlete, Ana Paula Oliveira, Denildo Magalhães, Márcio Magno, Márcio Teixeira, Sérgio Vitorino e Adérito.

A todos os colegas, técnicos administrativos e professores, da Escola Técnica de Saúde. Em especial, agradeço aos meus queridos amigos Clébio Domingues, Sheila Rodrigues, Tania Borges, Terezinha, Francisco, Fabiana Santos, Talita Mamed, Bruno Reis, Aline Bicalho, Juliana Faquim, Ludmila Mendonça, Samara Rodrigues, Noriel Vianna, Adriane Jansen, Claudia Cunha, Rose Santos, Rosa, Douglas, Mario Paulo Pennatti e Bia pela boa convivência e pelo carinho comigo.

Aos parceiros de pesquisa e grandes amigos João Lyra, Ubiratan, Polliana, Matheus, Isabella Cristina, Bruna Paes Leme, Leandro Miranda, Amanda Mazzaro, Raquel, Ludiel e Asbel. Com certeza nada disso seria realizado sem a parceria e dedicação de vocês. Obrigada pela contribuição impar de cada um nestes trabalhos. Obrigada por toda boa convivência, por cada sorriso, por cada dia ao lado de vocês. Serei eternamente grata!

A todos os meus colegas de doutorado, agradeço a oportunidade de tê-los conhecido e compartilhado desta caminhada com vocês. Valeu demais.

Aos amigos do Laboratório de Projetos Mecânicos, Alessandro, Artur, Carol, Denise, Fernando, Helton, Larissa, Lidiane, Marcília, Márcio, Mateus, José Eduardo Neto e Sérgio. Obrigada pela forma carinhosa como me receberam no laboratório, por toda a ajuda prestada no desenvolvimento deste trabalho, por todas as amizades construídas ao longo desses anos e por todos os bons momentos que pudemos compartilhar.

Ao engenheiro Dr. José Lúcio, que nos ajudou muito com o desenvolvimento destes trabalhos sempre com muito carinho e boa vontade. Obrigada, Zé, por tudo.

Ao pesquisador do Instituto Alberto Luiz Coimbra de Pós-Graduação e Pesquisa de Engenharia – UFRJ, Dr. Átila Teles. Agradeço pela grande

contribuição neste trabalho e por todos os ensinamentos na minha passagem pelo Rio de Janeiro. Serei sempre muito grata.

Às amigas que a odontologia e a pós-graduação me deram: Tatiane Gomes, Fabiane Maria, Luisa Cavalcante, Letícia Davi e Daniela Cristina. Vocês são especiais para mim. A caminhada, com certeza, foi mais prazerosa por poder dividi-la com vocês. E nossas tantas histórias, tantos momentos compartilhados eu guardo com muito carinho no meu coração. Amo muito vocês.

À minha querida amiga e colega de profissão Watuse. Você sempre foi uma das minhas maiores incentivadoras. Além de ser minha eterna colega de trabalho, será sempre uma das minhas melhores amigas. Deus foi generoso por nos permitir dividir nossas vidas, nossas famílias e nossas histórias. Meu amor e carinho serão sempre eternos e sinceros. Também não poderia deixar de agradecer ao Robson, pela amizade sincera e todo carinho comigo desde sempre. E claro, agradecer à nossa pequena princesa Astrid, sobrinha de coração, por me permitir amar de uma forma tão sincera e grandiosa.

Às minhas amigas de infância e adolescência, Ana Paula Rende, Carla Milken, Dayane Spirandelli, Gabriela do Vale, Julia Ferro, Juliana Cassiano, Karine Gomes, Karla Mendonça, Luna Ferolla, Olívia Félix, Patrícia Lacerda, Soraia El Kadi, Samira El Kadi e Vanessa Carvalho. Obrigada pelo amor e amizade que nos une há tantos anos. Obrigada por me apoiarem em todos os meus projetos pessoais e profissionais. Amo muito vocês!

Ao amigo Heltinho. Obrigada por nunca desistir de mim mesmo quando eu estava tão ausente. Obrigada por confiar no meu trabalho e na minha amizade. Você é muito especial. Você se foi antes de ler o que eu havia escrito aqui pra você, mas aí de cima sei que tem a certeza do que sempre significará pra mim.

À Ana Paula de Melo, obrigada por tudo. Você tem me ensinado, ao longo desses anos, a ver a vida por diferentes ângulos e isso tem sido genial. Com certeza, você contribuiu muito com a realização deste sonho.

À minha segunda família, Tia Cleide, Tio Marcelo, Ludmilla, Camilla e Marcelo Júnior. Obrigada por poder partilhar com vocês mais este momento. Obrigada por serem sempre presentes na minha vida.

À técnica em prótese dentária, Érica, por toda a ajuda, por partilhar comigo seus conhecimentos, por me auxiliar em tudo que preciso, por ser tão comprometida com o Curso Técnico de prótese e pela deliciosa convivência diária.

Aos técnicos do Laboratório de Projetos Mecânicos (LPM), Valdico (aposentado) e Diego, pela ajuda na confecção dos corpos de prova de tantos dos nossos trabalhos e pela presteza em sempre nos ajudar. E à técnica do laboratório de tribologia e materiais, Angela, por toda ajuda neste trabalho e pela alegria ímpar com que sempre nos recebeu no laboratório.

Às secretárias da pós-graduação Brenda e Graça. Obrigada por toda a dedicação com que realizam seus trabalhos nos ajudando sempre.

Aos alunos do curso de Prótese dentária da Escola Técnica de Saúde (ESTES), por toda boa convivência, por toda realização profissional que vocês me permitem alcançar, por todo o amor e carinho que têm por mim e por todo o aprendizado que tenho com vocês. Sem dúvida, vocês transformam meus dias de trabalho em dias de muita alegria.

Aos pacientes do projeto de extensão MASI, MP e PREPAD pela confiança no meu trabalho e pelo carinho que me tratam. Muito obrigada!

## **EPIÍGRAFE**

***“Sem a curiosidade que me move, que me inquieta, que me insere na  
busca, não aprendo nem ensino”***

***Paulo Freire***

## SUMÁRIO

RESUMO .....	16
ABSTRACT .....	17
1. INTRODUÇÃO E REFERENCIAL TEÓRICO .....	19
2. PROPOSIÇÃO .....	25
3. CAPÍTULOS.....	25
3.1. <i>Laser and plasma dental soldering techniques applied to Ti-6Al-4V alloy: Ultimate tensile strength and finite element analysis</i> .....	26
3.2. <i>Evaluation of TIG dental welding applied to Ti-6Al-4V alloys with different diameters: analysis by Ultimate Tensile Strength, Vickers Hardness, and Finite Element Method</i> .....	47
3.3. <i>Evaluation of X-shaped welded joints with Co-Cr alloy under different welding parameters: analysis by micro-CT and flexural strength</i> .....	66
3.4. <i>Maximum bite force measurement in patients subjected to different rehabilitation treatments – a pilot study</i> .....	82
4. DISCUSSÃO GERAL .....	93
5. CONCLUSÃO GERAL .....	100



## RESUMO

A reabilitação oral de pacientes totalmente edêntulos, especialmente a reabilitação de mandíbulas edêntulas, é uma realidade bem documentada e com extensos acompanhamentos longitudinais. Esse modelo de reabilitação, que ficou conhecido como 'protocolo de Branemark', tem sido motivo de vários estudos, tanto no que concerne aos implantes (número, distribuição, tratamento de superfície, tempos de carregamento, otimização do processo de osseointegração, dentre outros) quanto no que concerne à infraestrutura metálica. Os estudos voltados à infraestrutura metálica têm sido desenvolvidos no intuito de otimizar a confecção dessas por meio de barras pré-fabricadas e técnicas de soldagem alternativas à soldagem convencional. Nesse sentido, estudos vêm sendo realizados para avaliar os tipos de técnica de soldagem; as configurações dos equipamentos de soldagem; os tipos de ligas utilizados; as configurações das juntas e os métodos de avaliação mecânica dessas juntas. Assim sendo, foi proposto o presente trabalho, o qual compreende uma série de três artigos com o objetivo geral de avaliar as técnicas de soldagem Laser, TIG (Tungsten Inert Gas) e Plasma de uso odontológico aplicados às ligas de Co-Cr e Ti-6Al-4V com diferentes configurações de juntas e diferentes diâmetros, realizando as análises por meio de teste de tração, teste de flexão, dureza Vicker's, micro-CT e método de elementos finitos. O primeiro artigo tem por objetivo avaliar a resistência mecânica de estruturas de liga de Ti-6Al-4V em diferentes diâmetros com configuração da junta em I soldadas pelas técnicas laser e plasma de uso odontológico, por meio de teste de tração e análise por elementos finitos. O segundo artigo tem por objetivo avaliar a resistência mecânica de estruturas de liga de Ti-6Al-4V em diferentes diâmetros com configuração da junta em I soldadas pela técnica TIG, por meio de teste de tração, dureza Vicker's e análise por elementos finitos. O terceiro artigo tem por objetivo avaliar a resistência mecânica correlacionada com a porcentagem de volume total de solda e porosidades em juntas em X de liga de Co-Cr soldada com a técnica TIG com diferentes configurações do equipamento de soldagem, por meio de microtomografia computadorizada e teste de flexão. Para finalizar este trabalho, foi proposto um quarto artigo com o

objetivo de oferecer uma base clínica para comparação dos valores obtidos nos ensaios mecânico. Assim sendo, este último tem por objetivo avaliar a força máxima de mordida de dois tipos diferentes de reabilitação protética e comparar seus valores em indivíduos com oclusão normal e sem qualquer reabilitação protética.

**Palavras chaves:** Titânio, Soldagem, Ligas odontológicas, Resistência à tração, Método dos elementos Finitos, Força Máxima de Mordida.

## **ABSCTRAT**

Oral rehabilitation of edentulous patients, especially the rehabilitation of edentulous jaws, is a well-documented reality with extensive long-term follow up. This rehabilitation model, which became known as *ad modum* Branemark Protocol, has been the subject of several studies, both in relation to implants (number, distribution, surface treatment, load times, optimization of the osseointegration process, among others) as in relation to the metallic framework. The studies focused on prosthetic frameworks have been developed in order to optimize the production of these by prefabricated bars and alternative welding techniques to conventional welding. Studies have been conducted to evaluate the types of welding technique; the settings of welding equipment; the types of alloys used; the settings of the joints and mechanical methods of evaluation of these weld joints. Therefore, the following work was proposed which comprises a series of three articles with the overall objective to assess the laser, TIG (Tungsten Inert Gas) and Plasma dental welding techniques applied to Co-Cr and Ti-6Al-4V alloy with different settings joints and different diameters: analysis by means of tensile test, bending test, Vicker's hardness, micro-CT and finite element method. The first article proposed to evaluate the strength of Ti-6Al-4V alloy structures in different diameters with I-shaped joint configuration welded by laser and plasma techniques through tensile test and finite element analysis. The second article proposed to evaluate the strength of Ti-6Al-4V alloy structures in different diameters with I-shaped

joint configuration welded by TIG technique, through tensile testing, Vicker's hardness and finite element analysis. The third article proposed to evaluate the correlated mechanical strength with the percentage of total volume of solder and porosities of Co-Cr alloy X-shaped joint configuration welded by TIG technique with different settings of welding equipment, analyses by computed microtomography and bending test. To complete this work, a fourth article was proposed in order to provide a clinical basis for comparison of the values obtained in mechanical tests. Thus, the latter proposed to assess the maximum bite force of two different types of prosthetic rehabilitation and compare their values in subjects with normal occlusion and without any prosthetic rehabilitation.

**Keywords:** Titanium; Dental Soldering; Dental Alloys; tensile strength; Finite Element Method; Maximum Bite Force.

## 1- INTRODUÇÃO E REFERENCIAL TEÓRICO

A implantodontia voltada para a reabilitação oral de pacientes totalmente edêntulos é uma realidade bem documentada e extensivamente executada especialmente para mandíbulas edêntulas com altos índices de sucesso (Lyra e Silva et al., 2012; Castro et al., 2015). Esse modelo de reabilitação, que ficou conhecido como 'protocolo de Branemark', tem sido motivo de vários estudos, tanto no que concerne aos implantes quanto no que concerne à infraestrutura metálica (Berg et al., 1995; Wang and Welsh, 1995; Chai and Chou, 1998; Taylor et al., 1998; Baba and watanabe, 2005; Rocha et al., 2006; Watanabe and Topham, 2006; Zupanic et al., 2006; Akman et al., 2008; Byrne et al., 2011; Nunez-Pantoja et al., 2011; Barbi et al., 2012; Lyra e Silva et al., 2012; Nunez-Pantoja et al., 2012; Silveira-Júnior et al., 2012; Takayama et al., 2012; Atoui et al., 2013; Castro et al., 2013; Takayama et al., 2013; Bertrand et al., 2015; Castro et al., 2015; Kokolis et al., 2015; Matos et al., 2015; Simamoto-Júnior et al., 2015).

Os estudos voltados à infraestrutura protética têm sido desenvolvidos no intuito de otimizar a confecção dessas por meio de barras pré-fabricadas e técnicas de soldagem alternativas à soldagem convencional. (Berg et al., 1995; Wang and Welsh, 1995; Chai and Chou, 1998; Taylor et al., 1998; Baba and watanabe, 2005; Rocha et al., 2006; Watanabe and Topham, 2006; Zupanic et al., 2006; Akman et al., 2008; Byrne et al., 2011; Nunez-Pantoja et al., 2011; Barbi et al., 2012; Lyra e Silva et al., 2012; Nunez-Pantoja et al., 2012; Silveira-Júnior et al., 2012; Takayama et al., 2012; Atoui et al., 2013; Castro et al., 2013; Takayama et al., 2013; Bertrand et al., 2015; Castro et al., 2015; Kokolis et al., 2015; Matos et al., 2015; Simamoto-Júnior et al., 2015). Nesse sentido, estudos tem sido realizados para avaliar os tipos de técnica de soldagem (Wang and Welsh, 1995; Baba and Watanabe, 2004; Rocha et al., 2006; Zupanic et al., 2006; Barbi et al., 2012; Lyra e Silva et al., 2012; Nunez-Pantoja et al., 2012; Atoui et al., 2013; Castro et al., 2013; Castro et al., 2015; Matos et al., 2015; Simamoto-Júnior et al., 2015); as configurações dos equipamentos de soldagem (Chai and Chou, 1998; Baba and Watanabe, 2004, Akman et al.,

2008; Lyra e Silva et al., 2012); os tipos de ligas utilizados (Rocha et al., 2006; Watanabe and Topham, 2006; Lyra e Silva et al., 2012; Takayama et al., 2012; Takayama et al., 2013; Matos et al., 2015); as configurações das juntas (Zupanic et al., 2006; Nunez-Pantoja et al., 2012; Takayama et al., 2012; Takayama et al., 2013; Kokolis et al., 2015; Simamoto Júnior et al., 2015) e os métodos de avaliação mecânica dessas juntas (Nunez-Pantoja et al., 2011; Castro et al., 2015; Takayama et al., 2012; Takayama et al., 2013).

Dentre as possibilidades de confecção dessas infraestruturas, a técnica mais utilizada é aquela em que partes da barra são enceradas, fundidas e soldadas por meio de soldagem convencional ou brasagem (Berg et al., 1995; Wang and Welsh, 1995; Byrne, 2011; Silveira-júnior et al., 2012; Ghadhanfari et al., 2014). Esta técnica, embora utilizada durante muitos anos, é uma técnica que exige maior tempo de trabalho, tem um custo mais elevado de materiais e não é eficaz na soldagem do titânio e suas ligas (Lyra e Silva et al., 2012; Silveira-júnior et al., 2012). No entanto, técnicas mais precisas e simples podem ser utilizadas para atingir esses objetivos. Assim, além da utilização de barras pré-fabricadas (Lyra e Silva et al., 2012; Castro et al., 2015; Simamoto Júnior et al., 2015), as quais não necessitam ser fundidas, diferentes tipos de técnica de soldagem, como soldagem Laser (Berg et al., 1995; Neo et al., 1996; Chai e Chou, 1998; Baba and Watanabe, 2004; Rocha et al., 2006; Watanabe and Topham, 2006; Byrne, 2011; Kikuchi et al., 2011; Nuñez-Pantoja et al., 2011; Barbi et al., 2012; Ghadhanfari et al., 2014; Castro et al., 2015) e soldagens a arco - TIG (Tungsten Inert Gas) ou Plasma (Wag and Welsh, 1995; Neo et al., 1996; Chai e Chou, 1998; Taylor et al., 1998; Rocha et al., 2006; Byrne, 2011; Barbi et al., 2012; Castro et al., 2015; Simamoto Júnior et al., 2015) tem sido estudadas ao longo dos últimos 40 anos.

As soldagens TIG e plasma são processos nos quais a união é obtida pelo aquecimento dos materiais por um arco estabelecido entre o eletrodo não consumível de tungstênio e a peça a ser soldada, levando à fusão do metal base (Wang and Welsh, 1995; Neo et al., 1996; Taylor et al., 1998; Rocha et al., 2006; Byrne, 2011; Barbi et al., 2012; Nunez-Pantoja et al., 2012; Silveira-júnior et al., 2012; Atoui et al., 2013; Castro et al., 2013; Castro et al., 2015;

Simamoto-Júnior et al., 2015), o que permite a execução de soldas de alta qualidade e excelente acabamento, particularmente em juntas de pequena espessura (Silveira-júnior et al., 2012; Castro et al., 2015). Metal de adição pode ser utilizado ou não (Silveira-Júnior et al., 2012; Nunez-Pantoja et al., 2012; Matos et al., 2015; Simamoto Júnior et al., 2015). A proteção do eletrodo e da zona a ser soldada é feita por um gás inerte, normalmente o argônio ou mistura de gases inertes (Argônio e Hélio) (Wang and Welsh, 1995; Neo et al., 1996; Taylor et al., 1998; Rocha et al., 2006; Byrne, 2011; Barbi et al., 2012; Nunez-Pantoja et al., 2012; Silveira-júnior et al., 2012; Atoui et al., 2013; Castro et al., 2013; Castro et al., 2015; Simamoto-Júnior et al., 2015). O equipamento básico consiste de uma fonte de energia, uma tocha com eletrodo de tungstênio, uma fonte de gás de proteção e um sistema de abertura do arco. A principal diferença entre a solda TIG e a plasma é a utilização de um bocal constritor, na solda plasma, que causa a concentração do arco elétrico (Silveira-Júnior et al., 2012).

Já a soldagem laser é um processo de união baseado na fusão localizada da junta por meio de seu bombardeamento por um feixe de luz concentrada, coerente e monocromática de alta intensidade (Wang and Welsh, 1995; Neo et al., 1996; Fornaini et al., 2011; Castro et al., 2015). Uma das suas maiores vantagens é que ela produz um *Keyhole* que concentra a energia absorvida em uma pequena região, resultando em alta penetração (Roggensack et al., 1993; Wang and Welsh, 1995; Neo et al., 1996; Chai & Chou, 1998; Liu et al., 2002; Cho et al., 2003; Rocha et al., 2006; Akman et al., 2008; Srimaneepong et al., 2008; Nuñez-Pantoja et al., 2011, Silveira Júnior et al., 2012; Castro et al., 2015).

Ambas as técnicas têm algumas vantagens comuns, tais como: a soldagem pode ser efetuada diretamente sobre o modelo (Chai and Chou, 1998; Baba and Watanabe, 2004; Rocha et al., 2006; Zupanic et al., 2006; Kikuchi et al., 2011; Fornaini et al., 2011; Barbi et al 2012; Silveira-Júnior et al., 2012; Castro et al., 2015), a energia é concentrada em uma pequena área (Rocha et al., 2006; Barbi et al 2012; Lyra e Silva et al., 2012; Silveira-Júnior et al., 2012; Takayama et al., 2013; Castro et al., 2015), resultando em uma

reduzida Zona Afetada pelo Calor (ZAC) (Baba and Watanabe, 2004; Nunez-Pantoja et al., 2011; Silveira-Júnior et al., 2012; Castro et al., 2015) embora a soldagem laser resulte em uma ZAC ainda menor que a soldagem TIG (Atoui et al., 2013; Castro et al., 2015), ambas permitem a soldagem/reparo em regiões próximas à resina e cerâmica (Chai and Chou, 1998; Rocha et al., 2006; Watanabe and Topham, 2006; Zupanic et al., 2006; Nunez-Pantoja et al., 2011; Nunez-Pantoja et al., 2012; Silveira-Júnior et al., 2012; Castro et al., 2015; Kokolis et al., 2015), ambas permitem a soldagem em qualquer posição (Silveira-Júnior et al., 2012; Castro et al., 2015) e necessitam de menor tempo de trabalho que a soldagem convencional. (Baba and Watanabe, 2005; Rocha et al., 2006; Zupanic et al., 2006; Silveira-Júnior et al., 2012; Castro et al., 2015; Kokolis et al., 2015). A decisão sobre qual técnica de soldagem a ser utilizada é baseada mais na disponibilidade dos equipamentos nos laboratórios ou pela preferência individual do operador do que baseada em evidências científicas (Barbi et al., 2012). No entanto, o custo do equipamento é uma grande diferença entre as técnicas, sendo o equipamento de soldagem a laser muito mais caro do que o equipamento de soldagem TIG, o que, muitas vezes, impossibilita o uso do equipamento de solda laser nos laboratórios de prótese (Silveira Júnior et al., 2012; Atoui et al., 2013; Castro et al., 2015).

Independente do tipo de técnica utilizada, os estudos têm mostrado que a configuração do equipamento de solda parece exercer influência no processo de soldagem e no resultado final da junta soldada. Os estudos têm sido desenvolvidos no intuito de investigar a influência de alguns parâmetros de soldagem como, corrente ou voltagem (Chai and Chou, 1998; Baba and Watanabe, 2004; Akman et al., 2008; Kikuchi et al., 2011), duração do pulso (Chai and Chou, 1998; Baba and Watanabe, 2004; Akman et al., 2008; Kikuchi et al., 2011; Lyra e Silva et al., 2012; Takayama et al., 2013), o diâmetro do ponto de solda (Baba and Watanabe, 2004; Akman et al., 2008; Kikuchi et al., 2011; Takayama et al., 2013) e o uso dos gases de proteção (Akman et al., 2008; Watanabe and Topham, 2006; Takayama et al., 2012) na profundidade de penetração da solda.

Além disso, o tipo de liga também tem sido foco dos estudos (Rocha et al., 2006; Watanabe and Topham, 2006; Lyra e Silva et al., 2012; Takayama et al., 2012; Takayama et al., 2013). Embora o titânio e suas ligas sejam os mais utilizados nos estudos em virtude de algumas vantagens como boa compatibilidade, baixa densidade e propriedades anti-corrosivas (Berg et al., 1995; Chai and Chou 1998; Taylor et al., 1998; Rocha et al., 2006; Akman et al., 2008; Lyra e Silva et al., 2012; Nunez-Pantoja et al., 2011; Nunez-Pantoja et al., 2012; Silveira-Júnior et al., 2012; Takayama et al., 2012, Atoui et al., 2013; Takayama et al., 2013; Castro et al., 2015; Simamoto-Júnior et al., 2015), existe uma grande dificuldade em fundir e soldar essas ligas. Quando são submetidas a altas temperaturas, há uma grande reatividade dessas ligas com o oxigênio, o nitrogênio e o hidrogênio do ar, o que leva à sua contaminação, deixando as juntas soldadas mais fragilizadas. (Berg et al., 1995; Wang and Welsh, 1995; Chai and Chou, 1998; Taylor et al., 1998; Watanabe and Tophan, 2006; Akman et al., 2008; Lyra e Silva et al., 2012; Nunez-Pantoja et al., 2011; Nunez-Pantoja et al., 2012; Silveira-Júnior et al., 2012; Takayama et al., 2012; Atoui et al., 2013; Castro et al., 2015; Simamoto-Júnior et al., 2015). Somado a isso, as ligas de Co-Cr são cada vez mais populares para confecção de infraestruturas em prótese dentária. Essas ligas possuem uma combinação favorável de biocompatibilidade, resistência à corrosão, molhabilidade, rigidez e baixo custo (Rocha et al., 2006; Zupanic et al., 2006; Barbi et al., 2012; Kokolis et al., 2015).

A configuração da junta é outro fator que influencia a resistência das juntas soldadas (Nunez-Pantoja et al., 2011; Nunez-Pantoja et al., 2012; Takayama et al., 2013, Simamoto Júnior et al., 2015, Kokolis et al., 2015). Castro et al (2015) avaliaram a resistência mecânica de infraestruturas de liga de Ti-6Al-4V com amostras de diferentes diâmetros com a configuração da junta soldada em I soldadas pelas técnicas laser e plasma de uso odontológico e encontraram, em seus resultados, que houve uma incompleta penetração em todas as amostras dos grupos testes e que essa incompleta penetração pode ter sido a principal causa da diminuição da resistência das amostras. Resultados semelhantes foram encontrados por Zupanic et al. (2006) and



Kokolis et al (2015) em juntas soldadas com configuração em I de liga de Co-Cr soldadas com solda Laser. Além disso, Simamoto Junior et al, 2015, propuseram o uso de juntas soldadas com configuração em X ou chanfrada, sendo que isso melhorou muito o comportamento mecânico das juntas soldadas. A soldagem TIG associada com uma junta em X resultou em maior resistência das amostras. Além disso, no mesmo estudo, avaliaram dois ângulos diferentes desse tipo de chanfro e concluíram que tanto as amostras com um chanfro de 30 quanto com um de 45 graus apresentou melhores valores de resistência do que amostras sem chanfro.

Finalmente, os métodos de avaliação das juntas soldadas têm sido cada vez estudados no intuito de compreender o comportamento mecânico de estruturas soldadas e propor melhorias nos processos de soldagem. Portanto, muitos estudos têm utilizado métodos não-destrutivos, como inspeção radiográfica (Rocha et al., 2006; Nunez-Pantoja et al., 2011; Nunez-Pantoja et al., 2012; Simamoto-Júnior et al., 2015) e avaliação por líquidos penetrantes (Simamoto-Júnior et al., 2015) somados ou não aos métodos destrutivos como teste de resistência à tração (Berg et al., 1995; Wang and Welsh, 1995; Chai and Chou, 1998; Taylor et al., 1998; Watanabe and Topham, 2006; Zupanic et al., 2006; Akman et al., 2008; Takayama et al., 2012; Atoui et al., 2013; Takayama et al., 2013; Castro et al., 2015), teste de resistência à flexão (Rocha et al., 2006; Lyra e Silva et al., 2012; Atoui et al., 2013; Simamoto-Júnior et al., 2015) e teste de dureza Vicker's (Wang and Welsh, 1995; Takayama et al., 2012). Entretanto, poucos estudos têm sido realizados utilizando Microtomografia computadorizada (Micro-CT) (Takayama et al 2012; Takayama et al., 2013) e avaliação pelo método de elementos finitos (MEF) (Castro et al., 2015).

A avaliação por micro-CT possibilita a avaliação interna e tridimensional de toda a junta soldada, permitindo a identificação e o cálculo das porosidades e os vazios internos (Takayama et al., 2012; Takayama et al., 2013), bem como a avaliação de todo o volume de solda presente na região da junta. Já o MEF permite a utilização de modelos numéricos para verificação de tensões e deformações, comparáveis ou não aos testes mecânicos. Assim, soluções

aproximadas obtidas por este método podem elucidar o comportamento mecânico de determinadas estruturas soldadas (Castro et al., 2015).

Entretanto, se faz necessário uma base clínica para comparação dos valores obtidos nos ensaios mecânicos, tais como estudos em relação à força mastigatória exercida sobre estas estruturas já instaladas na boca dos pacientes. Neste cenário, estudos relacionados à força máxima de mordida (FMM) em diferentes tipos de aparelhos protéticos (Frauke et al., 2001; Caloss et al., 2011; Bilhan et al., 2012; Luraschi et al., 2012; Muller et al., 2012; Shah et al., 2012; Gonçalves et al., 2013; Al-Omiri et al., 2014; Gonçalves et al., 2014; Melo et al., 2016) poderiam, em partes, oferecer bases para esta comparação.

## **2. PROPOSIÇÃO**

O objetivo principal deste trabalho foi avaliar as técnicas de soldagem Laser, TIG e Plasma de uso odontológico aplicados às ligas de Co-Cr e Ti-6Al-4V com diferentes configurações de juntas e diferentes diâmetros por meio de teste de tração, teste de flexão, dureza Vicker's, micro-CT e método de elementos finitos. Além disso, objetiva estudar, de maneira preliminar, a força máxima de mordida de diferentes tipos de aparelhos protéticos para obtenção de bases iniciais de comparação para os valores obtidos nos testes mecânicos. Portanto, serão apresentados quatro artigos que, separadamente, abordarão esse objetivo principal.

## **3. CAPÍTULOS**

Serão apresentados nesta sessão quatro artigos separadamente sendo que cada um corresponde a um capítulo.

### **3.1. Laser and plasma dental soldering techniques applied to Ti-6Al-4V alloy: Ultimate tensile strength and finite element analysis**

Morgana G. Castro, DDS, MSc<sup>a</sup>; Cleudmar A. Araújo DDS, MSc, PhD<sup>b</sup>; Gabriela L. Menegaz, DDS, MSc<sup>c</sup>; João Paulo L. Silva, DDS, MSc<sup>d</sup>; Mauro Antônio A. Nóbilo, DDS, MSc, PhD<sup>e</sup>; Paulo César Simamoto Júnior DDS, MSc, PhD<sup>f</sup>

#### **ABSTRACT**

Statement of problem. The literature provides limited information regarding the performance of Ti-6Al-4V laser and plasma joints welded in prefabricated bars in dental applications. Purpose. The purpose of this study was to evaluate the mechanical strength of different diameters of Ti-6Al-4V alloy welded with laser and plasma techniques. Material and methods. Forty-five dumbbell-shaped rods were created from Ti-6Al-4V and divided into 9 groups (n=5): a control group with 3-mm and intact bars; groups PL2.5, PL3, PL4, and PL5 (specimens with 2.5-, 3-, 4-, and 5-mm diameters welded with plasma); and groups L2.5, L3, L4, and L5 (specimens with 2.5-, 3-, 4-, and 5-mm diameters welded with laser). The specimens were tested for ultimate tensile strength (UTS), and elongation percentages (EP) were obtained. Fractured specimens were analyzed by stereomicroscopy, and welded area percentages (WAP) were calculated. Images were made with scanning electron microscopy. In the initial analysis, the data were analyzed with a 2-way ANOVA (2×4) and the Tukey Honestly Significant Difference (HSD) test. In the second analysis, the UTS and EP data were analyzed with 1-way ANOVA, and the Dunnett test was used to compare the 4 experimental groups with the control group ( $\alpha=.05$ ). The Pearson and Spearman correlation coefficient tests were applied to correlate the study factors. Finite element models were developed in a workbench environment with boundary conditions simulating those of a tensile test. Results. The 2-way ANOVA showed that the factors welding type and diameter were significant for

the UTS and WAP values. However, the interaction between them was not significant. The 1-way ANOVA showed statistically significant differences among the groups for UTS, WAP, and EP values. The Dunnett test showed that all the tested groups had lower UTS and EP values than the control group. The 2.5 and 3.0 mm diameter groups showed higher values for UTS and WAP than the other test groups. A positive correlation was found between welded area percentage and ultimate tensile strength and a negative correlation between these parameters and the diameters of the specimens. No statistically significant difference was found between the weld techniques. Conclusions. Under the experimental conditions described, diameters of 2.5 and 3.0 mm resulted in higher UTS and WAP for both laser and plasma welding and appear to be the best option for joining prefabricated rods in this kind of union.

**Clinical implications.** Prefabricated bars and the plasma or laser welding technique are less time consuming and costly than the conventional technique and may be used to make implant frameworks for patients with an edentulous maxilla or mandible .

## INTRODUCTION

The rehabilitation of patients with edentulous mandibles with oral implants is a procedure with high success rates and an excellent long-term prognosis. Originally, treatments consisted of a 2-stage surgical protocol with 6 implants to support a fixed prosthesis. However, the protocol has gradually changed to a 1-stage surgical protocol with immediate loading.<sup>1</sup> Regardless of the delivery time of the prosthesis after implant placement, a series of procedures must be performed, and, because the bar must be waxed on the model, cast, and segmented and the parts indexed with resin and welded or brazed,<sup>2,3</sup> fabricating the metal framework is the most time consuming. One way to improve this process is to use prefabricated rods and new welding techniques.<sup>1</sup>

Currently, more than 50 different industrial welding techniques are used in areas such as aerospace, aviation, the automotive, petrochemical, and nuclear fields, medicine, and dentistry.<sup>6-16</sup> In dentistry, the most commonly technique available is gas-torch brazing (conventional welding). However other techniques and equipment can be used as alternatives to the conventional welding technique, including laser welding,<sup>3,6,7,9,10,12-23</sup> arc welding–tungsten inert gas (TIG),<sup>3,8,9,11,12,21</sup> and plasma welding.<sup>17,21</sup>

TIG and plasma welding are techniques in which union is achieved by heating the materials by establishing an arc between a nonconsumable tungsten electrode and the part to be welded.<sup>3,8,9,11,17</sup> The electrode and the area to be welded are protected by an inert gas, usually argon, or a mixture of inert gases (argon and helium).<sup>3,8,9,11,12,17</sup> Filler metal may be used. This technique produces high-quality welds and excellent finishing, especially in joints of small dimensions, and allows for welding in any position.<sup>24</sup>

Laser welding is a joining technique based on the localized fusion of the joint with bombardment by a beam of concentrated, coherent, and monochromatic high-intensity light.<sup>8,9,16</sup> One of its major advantages is that it produces a keyhole that concentrates the energy in a small region, resulting in high penetration and the formation of a narrow heat-affected zone (HAZ).<sup>4,5,8-10,12,15,17,18,23</sup> Ghadhanfari et al<sup>25</sup> compared the tensile strength obtained by the microwave postceramic soldering, conventional postceramic soldering, and laser postceramic welding of a gold-palladium metal ceramic alloy and found that the laser weld resulted in lower tensile strength values than the other techniques. They attributed this finding to the method used to prepare the joint area for a laser weld.

Although previous studies have investigated the mechanical properties, depths of penetration, and weld quality after laser welding,<sup>3,6,7,9,10,12,13,15-23</sup> arc welding–TIG, and plasma welding,<sup>3,8-12,17,21</sup> the welding conditions for different types of metals are not completely understood.<sup>10,14,15</sup> The purpose of this study was to evaluate the mechanical strength of Ti-6Al-4V alloy in different diameters subjected to laser welding (LW) and plasma welding (PW) techniques by applying the ultimate tensile strength (UTS) test and the finite element method

(FEM). The null hypotheses tested were that no difference would be found between the types of weld in relation to UTS, welded area percentage (WAP), and elongation percentage (EP); that increasing the diameters would not influence these 3 parameters (UTS, WAP, and EP); and that no difference would be found between the control and welded groups in terms of UTS and EP.

## **MATERIAL AND METHODS**

Forty-five dumbbell-shaped rods ( $n=5$ ) were machined from Ti-6Al-4V alloy (Realum; Indústria e Comércio de Metais Puros e Ligas Ltda) based on ASTM E 8 norm<sup>26</sup> with 2.5-, 3-, 4-, and 5-mm diameters in the central segment. The specimen size was obtained from a specimen calculation in the SigmaPlot program, with a 0.9 power of analysis. The specimens were machined into halves to be welded later in the LW machine (Desktop; Dentauro JP Winkelstroter KG) or in a PW machine (Micromelt; EDG); those belonging to the control group (CG) were machined intact. The specimens were divided into 9 groups: CG, PL2.5, PL3, PL4, and PL5 (specimens welded by PW) and L2.5, L3, L4, and L5 (specimens welded by LW).

The specimen halves were aligned in the metal matrix so that the parts to be welded were completely abutting to allow the standardization of the welding position for all groups. The LW machine uses a Nd:YAG crystal as a light source and was adjusted for 365 V and a 9-ms pulse. The focus and frequency were calibrated at 0, and the welding was performed by the same operator (Nóbilo MAA) at one time. The PW machine was adjusted for working with a 10 A depth (current density) and 3-ms pulse (continuous arc), and the welding was performed by the same operator (Simamoto Júnior PC) at one time. For both techniques, 2 opposite points of welding were marked to stabilize the specimens. Then the framework was removed from the matrix to facilitate the welding of the entire circumference.

The UTS measurement was carried out in a universal testing machine (MTS 810; Material Test System Corp) at a crosshead speed of 0.02 mm/min

and 2.500 KGF load cell. The UTS (MPa) was recorded when the specimens fractured and the EP was obtained by subtracting the final length from the initial length and dividing the result by the initial length. The initial length was obtained after welding and was measured with a digital caliper. The final length was measured by positioning the correct halves of the specimens fractured after UTS testing in the metal matrix so that fractures remained juxtaposed; this was also measured with a digital caliper. Percentages were obtained when the differences were multiplied by 100.

After the UTS test, both parts of the fractured specimens were evaluated by stereomicroscopy (Leica MS5; Leica Microscopy Systems) with  $\times 2.5$  magnification for the 2.5- and 3-mm diameters and  $\times 1.6$  for the 4- and 5-mm diameters. The captured images were analyzed with Motic Images Plus 2.0 software for Windows (Motic; Richmond). All areas ( $\text{mm}^2$ ) were measured and tabulated. The average for each specimen and then the average for all specimens were calculated. The values obtained were converted to percentages so that the different diameters could be compared.

Since the specimens in each group had similar fracture patterns, 3 specimens of each diameter were subjected to SEM with  $\times 25$ ,  $\times 100$ , and  $\times 500$  magnification, and those images that were most representative were used to demonstrate the welded penetration area and the failure characteristic (JSM 5600LV; JEOL).

Three-dimensional FE models based on the original 3.0-mm specimens used in the experimental analysis (UTS) were constructed by computer-aided design (CAD) software (Solidworks; Dassault Systems) for both intact and welded specimens. All models were then transferred to FE processing software (Ansys Workbench 12.0; Ansys).

To ensure consistency and accuracy in the simulations for this study, all FE models had similar mesh densities, with higher node density in all regions of the specimens. The 3D models contained a total of 2202 elements and 4699 nodes for nonwelded specimens, 3270 elements and 6993 nodes for laser-welded specimens, and 3740 elements and 7907 nodes for plasma-welded specimens.

All materials were assumed to behave with linear elasticity. The mechanical properties (Young modulus and Poisson ratios) for the base material were obtained from the software itself. The Young modulus was increased about 20% for the weld area. This estimation of 20% increase was used because the literature reports that hardness is increased in this region.<sup>8,17</sup> The boundary conditions were defined primarily in constraints on displacement of a side face of the structure, that is, with part of the template clamped (fixed) without freedom of movement. The loading configuration followed that of the UTS analysis, with its direction parallel to the Z axis. The strength values used were obtained from the UTS test. After the processing step, data were obtained on displacement on the Z axis (mm) and on maximum principal stress (MPa).

Model validation was performed for the intact specimen. The values of the force applied in the UTS intact specimens were used as a reference for computer simulation. Displacement and stress values of the numerical models were then compared with the displacement and stress values of the experimental group. Stress × deformation curves were close, so the FE model was validated.

In the initial analysis, the goal was to determine the influence of the 2 factors involved in this study: type of weld and diameter. Therefore, the data were analyzed with a 2-way ANOVA (2×4) and the Tukey Honestly Significant Difference (HSD) test. In the second analysis, the UTS and EP data were analyzed with 1-way ANOVA, and the Dunnett test was used to compare the 4 experimental groups with the control group ( $\alpha=.05$  for all tests). Subsequently, the Pearson correlation test was performed to correlate UTS with WAP, and the Spearman correlation test was performed to correlate the diameters of the specimens with UTS and the diameters with WAP.

The data found in the FE analysis were analyzed by direct comparative models generated for different welding processes in relation to the model generated for the intact specimen and between the experimental and numerical models. At this time, in the MEF, the term 'experimental' was used to designate specimens that were subjected to the UTS test, whether or not they were welded.



## RESULTS

Mean and standard deviation values for the UTS (MPa) in each tested group, with and without the control group, are shown in Tables I and II. The 2-way ANOVA showed that factors welding type ( $P=.012$ ) and diameter ( $P<.001$ ) were significant for the UTS values. However, the interaction between them ( $P=.623$ ) was not significant (Table III). The Tukey test showed that the UTS values of the specimens with 2.5 mm diameters were significantly higher than those of the specimens with 4.0 mm ( $P=.012$ ) and 5.0 mm diameters ( $P<.001$ ), irrespective of the welding type. The 1-way ANOVA showed significant differences among the groups for UTS values ( $df=8$ ,  $F=23.86$ ,  $P<.001$ ). The Dunnett test showed that all the tested groups had lower UTS values than those of the control group (Table II).

**Table I.** Mean and standard deviations (SD) for ultimate tensile strength (MPa), welded area (%) and elongation (%), and statistical categories defined by Tukey test.

Diameter	Ultimate Tensile Strength (MPa)		Welded Area Percentage (%)		Elongation Percentage (%)	
	Mean $\pm$ SD		Mean $\pm$ SD		Mean $\pm$ SD	
	Laser	Plasma	Laser	Plasma	Laser	Plasma
2.5	762.9 $\pm$ 133.6 <sup>Aa</sup>	627.3 $\pm$ 94.2 <sup>Ba</sup>	73.2 $\pm$ 8.0 <sup>Aa</sup>	47.9 $\pm$ 5.2 <sup>Ba</sup>	1.9 $\pm$ 1.9 <sup>Ab</sup>	1.6 $\pm$ 1.0 <sup>Ab</sup>
3.0	601.9 $\pm$ 232.9 <sup>Aab</sup>	571.5 $\pm$ 108.6 <sup>Bab</sup>	70.9 $\pm$ 8.0 <sup>Aa</sup>	43.8 $\pm$ 6.2 <sup>Ba</sup>	1.1 $\pm$ 0.8 <sup>Ab</sup>	1.4 $\pm$ 0.9 <sup>Ab</sup>
4.0	542.8 $\pm$ 179.9 <sup>Ab</sup>	434.8 $\pm$ 79.6 <sup>Bb</sup>	56.0 $\pm$ 2.8 <sup>Ab</sup>	36.7 $\pm$ 4.7 <sup>Bb</sup>	1.0 $\pm$ 0.3 <sup>Ab</sup>	0.4 $\pm$ 0.3 <sup>Ab</sup>
5.0	515.6 $\pm$ 154.2 <sup>Ab</sup>	320.6 $\pm$ 38.7 <sup>Bb</sup>	52.6 $\pm$ 7.5 <sup>Ac</sup>	26.6 $\pm$ 1.8 <sup>Bc</sup>	0.8 $\pm$ 0.3 <sup>Ab</sup>	1.6 $\pm$ 0.9 <sup>Ab</sup>

Different capital letters represent significant difference identified by Tukey HSD test for welding type in each parameter ( $P<.05$ ). Different lowercase letters represent significant difference identified by Tukey HSD test for diameters of specimen in each weld and each parameter.

**Table II.** Mean fracture resistance values (N) and standard deviations (SD) ultimate tensile strength (MPa), and elongation values (%), of control and experimental groups (n=5), and P values calculated by Dunnett test.

	Ultimate Tensile	P	Elongation	P
Group	Strength (MPa)		Percentage (%)	
CG	1008.5 ±37.1 <sup>a</sup>	-	7.5 ±1.2 <sup>A</sup>	-
L2.5	762.9 ±133.6 <sup>b</sup>	=.036	1.9 ±1.9 <sup>B</sup>	<.001
L3.0	601.9 ±232.9 <sup>b</sup>	<.001	1.1 ±0.8 <sup>B</sup>	<.001
L4.0	542.8 ±179.9 <sup>b</sup>	<.001	1.0 ±0.3 <sup>B</sup>	<.001
L5.0	515.6 ±154.2 <sup>b</sup>	<.001	0.8 ±0.3 <sup>B</sup>	<.001
PL2.5	627.3 ±94.2 <sup>b</sup>	<.001	1.6 ±1.0 <sup>B</sup>	<.001
PL3.0	571.5 ±108.6 <sup>b</sup>	<.001	1.4 ±0.9 <sup>B</sup>	<.001
PL4.0	434.8 ±79.6 <sup>b</sup>	<.001	0.4 ±0.3 <sup>B</sup>	<.001
PL5.0	320.6 ±38.7 <sup>b</sup>	<.001	1.6 ±0.9 <sup>B</sup>	<.001

\*Data were analyzed by 1-way ANOVA and Dunnett test ( $\alpha=.05$ )

**Table III.** Two-way ANOVA (2×4) for ultimate tensile strength values (MPa) of welded groups

Source of variation	Df	Sum of square	Mean square	F	P
Welding	1	137442	137442	7.011	.012
Diameter	3	435284	145094	7.402	<.001
Welding x diameter	3	35020	11673	0.596	.623
Residual	32	627286	19602		
Total	39	1235033	31667		

Mean and standard deviation values for the WAP (%) in each tested group are shown in Table I. For WAP, the factors welding type ( $P<.001$ ) and diameter ( $P<.001$ ) were significant. However the interaction between them ( $P=.178$ ) was not significant as shown by the 2-way ANOVA (Table IV). The WAP values of the specimens with 2.5 mm and 3.0 mm diameters were significantly higher than specimens with 4.0 mm diameters ( $P<.001$ ), the specimens with 2.5 mm and 3.0 mm diameters were also significantly higher than specimens with 5.0 mm diameters ( $P<.001$ ), and the specimens with 4.0 mm diameters were significantly higher than those with 5.0 mm diameters ( $P=.003$ ), irrespective of the welding type.

**Table IV.** Two-way ANOVA (2×4) for welded area values (%) of welded groups

Source of variation	df	Sum of square	Mean square	F	P
Welding	1	11934	11934	336.603	<.001
Diameter	3	5677	1892	53.376	<.001
Welding x diameter	3	179	59	1.683	.178
Residual	72	2552	35		
Total	79	20344	257		

Mean and standard deviation values for the EP (%) in each tested group with and without the control group are shown in Tables I and II. For EP, the factors type of welding ( $P=.861$ ) and diameter ( $P=.185$ ) and the interaction between them ( $P=.475$ ) were not significant as shown by the 2-way ANOVA

(Table V). For EP values, the 1-way ANOVA showed significant differences among the groups and control group ( $df=8$ ,  $F=11.04$ ,  $P<.001$ ). The Dunnett test showed that all tested groups had lower EP values than the control group (Table V).

**Table V.** Two-way ANOVA ( $2 \times 4$ ) for elongation values (%) of welded groups

Source of variation	df	Sum of square	Mean square	F	P
Welding	1	0.0296	0.0296	0.0310	.861
Diameter	4	6.339	1.585	1.660	.185
Welding x diameter	4	3.444	0.861	0.902	.475
Residual	30	28.644	0.955		
Total	39	38.452	0.986		

Figures 1 and 2 are SEM images of the fractured welded area of the LW specimens, and Figure 3 is an SEM image of the fractured welded area of a PW specimen. Figure 1 shows that a major portion of the central area was not joined. Figures 2 and 3 show the fracture in the Ti-6Al-4V material after LW and PW. Both presented a fairly flat overall surface with shallow dimples, indicating a small amount of ductility. In addition, many voids and porosities were found in the welded area.

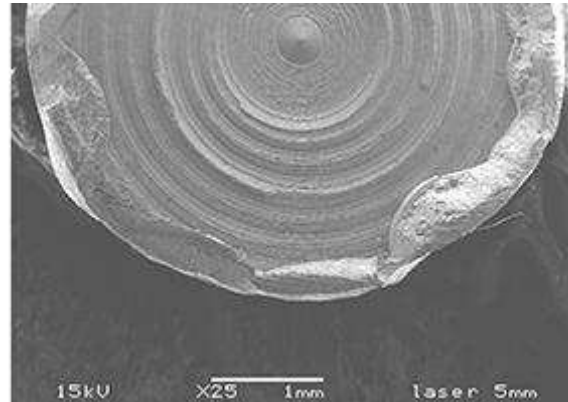


**Figure 1.** Scanning electron microscope image at  $\times 25$  magnification of specimen from L5 group.

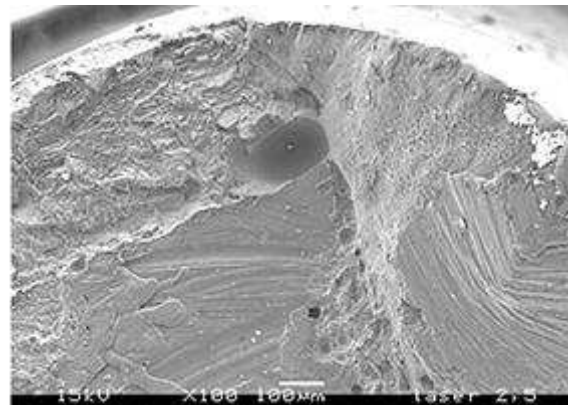


**Figure 2.** Scanning electron microscope images at  $\times 100$  magnification of specimen from L2.5 group.

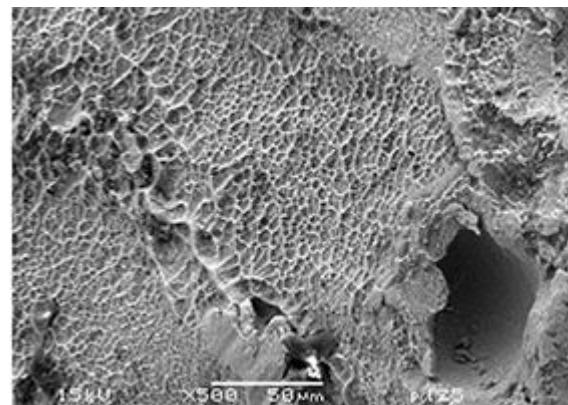


**Figure 3.** Scanning electron microscope images at  $\times 100$  magnification of specimen from PL2.5 group.

The Pearson correlation test showed that the higher the UTS, the higher the WAP for both LW (.472) and PW (.981). The Spearman correlation test demonstrated that the smaller the diameter, the higher the WAP for both LW (-.807) and PW (-.869). The Spearman correlation test also demonstrated that the smaller the diameter, the higher the UTS for both LW (-.535) and PW (-.830).

The values obtained from the FE models were compared with the values from the experimental models for directional deformation on the Z axis for both the intact specimens and for specimens welded with PW and LW to a 3-mm diameter for selected displacements.

The stress-strain graph of the control group (Fig. 4) shows that the curves of both the experimental groups and the FE model were close. For both the laser and plasma experimental groups, the graph (Fig. 5) shows that the curves of both the experimental group and the FE model were close. However, more adjustments to the FE model in terms of geometry and the properties of the material in the weld area are necessary so that these curves might be even closer. Although these are beginning models to be used with welded structures, they can be taken as representative of LW and PW techniques. Moreover, stress concentration can be seen throughout the central body (Fig. 6), showing that fracture can occur at any point in this region.

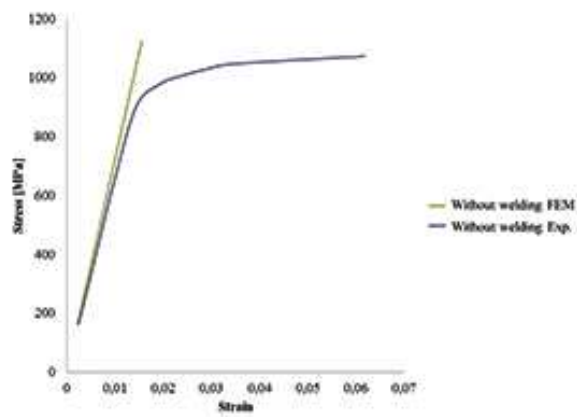


**Figure 4.** Stress × deformation curve of nonwelded specimens.

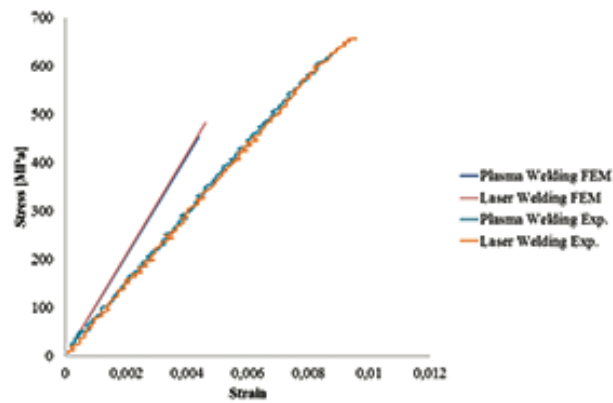


**Figure 5.** Stress × deformation curve of welded specimens.

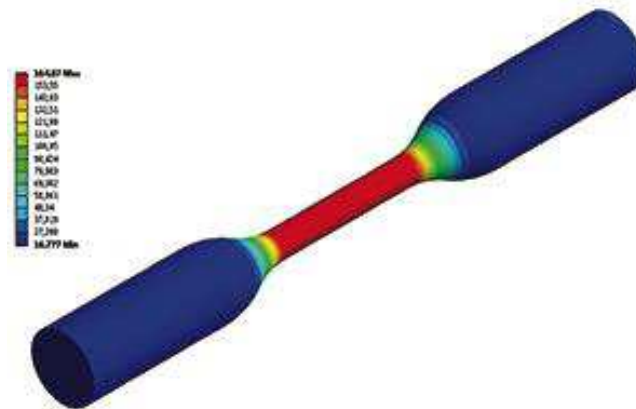


**Figure 6.** Model showing stress concentrations throughout central body.

## DISCUSSION

The 3 null hypotheses were rejected. The first null hypothesis was that no difference would be found between the types of weld in relation to UTS, WAP, and EP. The statistical analysis showed that the factor 'type of welding' was significant for the UTS ( $P=.012$ ) and WAP ( $P<.001$ ) values (Tables III and IV). However, the factor 'type of welding' ( $P=.861$ ) was not significant in relation to EP (Table V).

In both parameters (UTS and WAP), the LW had higher values than the PW. Adequate energy delivery to areas to be joined, method of energy delivery, and cooling rate are some factors that affect Ti joining and should be considered. Thus, the LW shows some differences in relation to PW, such as a smaller HAZ, faster cooling cycle, and highly localized energy.<sup>8</sup> These differences could influence the results.

Furthermore, because the tungsten electrode must be sharpened before each weld, working with PW is difficult. If the electrode is not sharpened according to the specifications of the PW equipment, a good-quality weld cannot be achieved. Tungsten electrode pointers that streamline this step and ensure proper electrode sharpening are available.

Conversely, regardless of the outcome, both techniques have similar advantages. They may be welded on the cast itself, they allow for welding in areas close to resin or porcelain,<sup>3,10,14-16,24</sup> they allow for welding in any position, and they require less time than conventional welding.<sup>12,20,24</sup>

The second null hypothesis was that increased diameter would not influence the parameters analyzed (UTS, WAP, and EP). Statistical analysis by



2-way ANOVA showed that the factor 'diameter' was significant for UTS ( $P<.001$ ) and WAP ( $P<.001$ ) values (Tables III and IV). However, the factor 'diameter' ( $P=.185$ ) was not significant in relation to EP (Table V). Also, the Tukey test showed statistically significant differences between the diameters for UTS and WAP, but not for EP (Table I).

In the analyses of the UTS and WAP by the Tukey test, specimens with smaller diameters had the highest values, regardless of the type of welding (Table I). A negative correlation was found between WAP and the diameter of the specimen for both LW (-.807) and PW (-.869). A negative correlation was also found between the diameter of the specimen and the UTS for both LW (-.535) and PW (-.830). Therefore, the increased diameters had a negative influence on the UTS and the WAP of the specimens.

However, these values were obtained with the same machine settings, 10 A and 3 ms for PW and 365 V and 9 ms for LW. The energy level of the LW can be controlled by parameters such as current or voltage, pulse duration, and diameter of the spot weld.<sup>5,10,14</sup> Some authors<sup>10,14,18,20,22</sup> have reported that the depth of penetration, LW to titanium, was proportional to current or voltage and that the UTS was significantly influenced by this parameter. Thus, for best results, especially for larger diameters, the regulation of the equipment is critical.<sup>9,14,17,18,20</sup> Despite the existence of numerous studies of LW, a protocol for welding has not been established.<sup>10,14,15</sup>

Another factor that could have influenced these results is joint configuration. The joint used in this study does not appear to be the best, particularly for larger diameters (4 and 5 mm), because of the limited heat input

of welding machines designed for dentistry. Another project using an X-shaped joint-type may be developed, since, in the shape of the X gasket, the center is kept juxtaposed, allowing for weld penetration depth.<sup>15</sup>

The third null hypothesis was that no difference would be found between the control group and the welded groups in relation to UTS and EP. One-way ANOVA showed statistically significant differences among all groups for both parameters, and the Dunnett test showed that the test groups presented lower UTS and EP than did the control group (Table II).

One factor that contributed to this result is that the processes for electric arc welding are characterized by the imposition of large amounts of directed heat to achieve fusion of the filler and the base material.<sup>3,8,9,11,17</sup> This causes significant microstructural transformations in the HAZ of the base metal, whose structure or properties were changed by variations in temperature during welding.<sup>28</sup> These changes create a complex array of stress and strain, leading to distortion of the material, residual stresses, generation of fragile microstructures, grain growth, cracks, and changes in mechanical, physical, and chemical properties.<sup>27</sup>

Similarly, the joints welded by LW also suffer from defects that result from residual stress. Typically, residual stress introduced in the weld joints is a consequence of the thermal stress caused by cycles of heating and cooling of the welding process. Therefore, it affects the mechanical behavior of the LW structures.<sup>4</sup>

Another factor is that titanium reaches temperatures where the metal has a high affinity with elements such as oxygen, hydrogen, and nitrogen. These are

added to its structure, making it rich in impurities, which reduce its ductility and UTS values,<sup>7,8,10,11,13,17</sup> even though it is welded in a welding machine with inert gas protection.

In addition to these factors, the presence of bubbles and porosities due to the inclusion of argon gas during the welding procedure should be considered.<sup>5,13,15,17-19</sup> These bubbles and porosities act as fracture initiators, since they function as stress concentration points and can quickly lead to the failure of the welded structure under the application of forces lower than those needed to damage the adequate joint.<sup>9</sup> In the SEM images (Figs. 2 and 3), several areas of porosity can be identified.

Conversely, the lowest UTS values for the experimental groups are the result of incomplete union penetration.<sup>8,9,14,17,19</sup> According to some authors,<sup>10,18-20</sup> the penetration depth of the weld is the main factor affecting the resistance values of the LW structures. In this study, a positive correlation was found between WAP and UTS values for both LW (.472) and PW (.981), showing that penetration is a factor to be considered in the values of UTS. When the weld penetration is insufficient, a large bubble or internal fault occurs,<sup>15,20</sup> particularly in the larger diameter, leaving the welding confined to the border of the specimen.

A limitation of this study was the lack of information regarding the longevity of the welding procedures. In future studies, nondestructive testing with microcomputed tomography (Micro-CT) and radiographic inspection should be combined with other destructive tests.

Although the Ti-6Al-4V alloy was used in this study because of its favorable chemical, biological, and mechanical properties,<sup>8,10,11,15,18</sup> other alloys can be evaluated and the results used for comparison with those obtained in this investigation.

## **CONCLUSIONS**

Within the limitations of this research, the diameters of 2.5 and 3.0 mm showed the highest values of UTS and WAP and seem to be the best options for joining prefabricated bars in prosthetic frameworks both with PW and LW, in terms of machine regulation, and in terms of the configuration of the joint used in this study.

## **REFERENCES**

1. Hatano N, Yamaguchi M, Yaita T, Ishibashi T, Sennerby L. New approach for immediate prosthetic rehabilitation of the edentulous mandible with three implants: a retrospective study. Clin Oral Implants Res 2011;22:1265-9.
2. Anusavice KJ, Shen C, Rawls HR. Phillips' science of dental materials. 12th ed. St. Louis: Elsevier, Saunders; 2013. p. 367-95.
3. Barbi FC, Camarini ET, Silva RS, Endo EH, Pereira JR. Comparative analysis of different joining techniques to improve the passive fit of cobalt-chromium superstructures. J Prosthet Dent 2012;108:377-85.
4. Cho S-K, Yang Y-S, Son K-J, Kim J-Y. Fatigue strength in laser welding of the lap joint. Finite Elem Anal Des 2004;40:1059-70.

5. Akman E, Demir A, Canel T, Sinmazçelik T. Laser welding of Ti6Al4V titanium alloy. *J Mater Proc Technol* 2009;209:3705-13.
6. Sjögren G, Andersson M, Bergman M. Laser welding of titanium in dentistry. *Acta Odontol Scand* 1988;46: 247-53.
7. Berg E, Wagnere WC, Davik G, Dootz ER. Mechanical properties of laser-welded cast and wrought titanium. *J Prosthet Dent* 1995;74:250-7.
8. Wang RR, Welsch GE. Joining titanium materials with tungsten inert gas welding, laser welding, and infrared brazing. *J Prosthet Dent* 1995;74:521-30.
9. Neo TK, Chai J, Gilbert JL, Wozniak WT, Engelman MJ. Mechanical properties of titanium connectors. *Int J Prosthodont* 1996;9:379-93.
10. Chai T, Chou CK. Mechanical properties of laser-welded cast titanium joints under different conditions. *J Prosthet Dent* 1998;79:477-83.
11. Taylor JC, Hondrum SO, Prasad A, Brodersen CA. Effects of joint configuration for the arc welding of cast Ti-6Al-4V alloy rods in argon. *J Prosthet Dent* 1998;79:291-7.
12. Rocha R, Pinheiro AL, Villaverde AB. Flexural strength of pure Ti, Ni-Cr and Co-Cr alloys submitted to Nd:YAG laser or TIG welding. *Braz Dent J* 2006;17:20-3.
13. Watanabe I, Topham DS. Laser welding of cast titanium and dental alloys using argon shielding. *J Prosthodont* 2006;15:102-7.
14. Kikuchi H, Kurotani T, Kaketani M, Hiraguchi H, Hirose H, Yoneyama T. Effect of laser irradiation conditions on the laser welding strength of cobalt-chromium and gold alloys. *J Oral Sci* 2011;53:301-5.

15. Nuñez-Pantoja JM, Vaz LG, Nóbilo MA, Henriques GE, Mesquita MF. Effects of laser-weld joint opening size on fatigue strength of Ti-6Al-4V structures with several diameters. *J Oral Rehabil* 2011;38:196-201.
16. Fornaini C, Passaretti F, Villa E, Rocca JP, Merigo E, Vescovi P, *et al*. Intraoral laser welding: ultrastructural and mechanical analysis to compare laboratory laser and dental laser. *Lasers Med Sci* 2011;26:415-20.
17. Roggensack M, Walter MH, Böning KW. Studies on laser- and plasma-welded titanium. *Dent Mater* 1993;9:104-7.
18. Liu J, Watanabe I, Yoshida K, Atsuta M. Joint strength of laser-welded titanium. *Dent Mater* 2002;18:143-8.
19. Zavanelli RA, Guilherme AS, Pessanha-Henriques GE, de Arruda Nóbilo MA, Mesquita MF. Corrosion-fatigue of laser-repaired commercially pure titanium and Ti-6Al-4V alloy under different test environments. *J Oral Rehabil* 2004;31:1029-34.
20. Baba N, Watanabe I. Penetration depth into dental casting alloys by Nd:YAG laser. *J Biomed Mater Res B Appl Biomater* 2005;72:64-8.
21. Hart CN, Wilson PR. Evaluation of welded titanium joint used with cantilevered implant-supported prostheses. *J Prosthet Dent* 2006;96:25-36.
22. Lin MC, Lin SC, Wang YT, Hu SW, Lee TH, Chen LK, *et al*. Fracture resistance of Nd:YAG Laser-welded cast titanium joints with various clinical thicknesses and welding pulse energies. *Dent Mater J* 2007;26:367-72.
23. Srimaneepong V, Yoneyama T, Kobayashi E, Doi H, Hanawa T. Comparative study on torsional strength, ductility and fracture characteristics of

laser-welded alpha+beta Ti-6Al-7Nb alloy, CP titanium and Co-Cr alloy dental castings. *Dent Mater* 2008;24:839-45.

24. Silveira-Júnior CD, Castro MG, Davi LR, Neves FD, Novais VR, Simamoto-Júnior PC. Welding techniques in dentistry. In: Kovacevic R, editor. *Welding Processes*. 17<sup>th</sup> ed. Croatia: In tech;2012, p.415-38.

25. Ghadhanfari HA, Khajah HM, Monaco Jr EA, Kim H. Effects of soldering methods on tensile strength of a gold-palladium metal ceramic alloy. *J Prosthet Dent* 2014;J Prosthet Dent 2014 May 16. [Epub ahead of print].

26. American Welding Society. Standard methods for mechanical testing of welds. ANSI/AWS B4.0-92. Specification: E 8M – 04: Standard test methods for tension testing of metallic materials. Miami: American Welding Society;1998. p. 15-23.

27. Meadows C, Fritz JD. Understanding stainless steel heat-affected zones. *Welding J* 2005;26-30.

28. Ramirez JE, Mishael S, Shockley R. Properties and sulfide stress cracking resistance of coarse-grained heat-affected zones in V-microalloyed X60 steel pipe. *Welding J* 2005;113-23.

### **3.2. Evaluation of TIG dental welding applied to Ti-6Al-4V alloys with different diameters: analysis by Ultimate Tensile Strength, Vickers Hardness, and Finite Element Method**

Morgana G. Castro, DDS, MS<sup>a</sup>; Cleudmar A. Araújo DDS, MS, PhD<sup>b</sup>; Gabriela L. Menegaz, DDS, MS<sup>c</sup>; Mattheus B. Santos, DDS, MS<sup>d</sup>; Washington M. Silva Júnior, DDS, MS, PhD<sup>e</sup>; Paulo César Simamoto Júnior DDS, MS, PhD<sup>f</sup>

#### **ABSTRACT**

Statement of the problem: There is limited information in literature regarding the accomplishment of Ti-6Al-4V TIG joints welded in prefabricated bars applied to dentistry. Purpose: Evaluate the ultimate tensile strength and Vickers hardness of Ti-6Al-4V alloy subjected to TIG (Tungsten Inert Gas) welding technique in different diameters. Material and methods: Forty-five specimens were prepared and divided into 5 groups: control group (CG) (n=5), with intact bars in a diameter of 3.0mm, and groups TIG2.5, TIG3, TIG4, TIG5 (n=10) with diameters of 2.5, 3, 4 and 5 mm respectively, welded with TIG in a pulse of 10(ms) and in a depth of 3(A). The specimens were tested by both radiographic inspection and penetrating liquids. After that, they were tested by ultimate tensile strength (UTS) and the elongation percentage (EP) was obtained. Images from fractured samples were taken and the welded areas percentage (WAP) was calculated. Random images were also taken by scanning electron microscope (SEM). Vickers hardness was obtained for base metal (BM), Heat affected zone (HAZ) and Welded zone (WZ). Finite element models were constructed. One-way Anova, Dunnet and Tukey tests ( $\alpha=.05$ ) were used for statistical analysis of UTS, WAP and EP for different groups and for differences in regions (BM, HAZ and WZ). Finite element models were developed in a workbench environment with boundary conditions simulating a tensile test. Results: The majority of the specimens showed internal voids on radiographic



inspection, but porosities or grooves were not observed on there surface on penetrant liquid test. Most of the samples fractured in the welded area. The 1-way ANOVA showed significant differences among the groups for UTS values ( $P<.001$ ), for WAP values ( $P<.001$ ) and for EP values ( $P<.001$ ). The Dunnett test showed that TIG3, TIG4 and TIG5 groups had lower UTS values than those of the CG, but TIG2.5 group had no statistical difference in relation to CG. The 1-way ANOVA showed significant differences among the regions ( $P<.001$ ) for Vickers hardness. Conclusion: Under the experimental conditions described, the diameter of 2.5 seems to be the best option for joining prefabricated rods in this kind of union and in this regulation of the machine.

Keywords: Dental Soldering, scanning electron microscopy, tensile strength, titanium alloy

**CLINICAL IMPLICATIONS:** Prefabricated bars and the Tungsten Inert Gas (TIG) welding technique may be used to make or repair implant frameworks for patients with an edentulous maxilla or mandible.

## INTRODUCTION

The rehabilitation of edentulous jaws through prostheses fixed on implants of the *ad modum* Brånemark Protocol type has been well-documented, with high success rates.<sup>1,2</sup> The focus of this study was on establishing this type of rehabilitation more quickly and more cost-effectively, for both professionals and patients.<sup>1-4</sup> Several investigators have studied implants, and others have assessed the metallic structures.<sup>1-24</sup>

The studies related to frameworks have focused on: welding technique types<sup>1,2,4,6,7,10,11,16,17,19,20,22</sup>; the settings of welding equipment<sup>1,8,10,13</sup>; the types of alloys used<sup>1,11,12,18,21,22</sup>; the configuration of the joints<sup>4,17,18,21,24</sup>; and mechanical methods of evaluation of these welded joints.<sup>2,15,18,21</sup>

Among the possible approaches to creation of the framework, the most used technique is one in which parts of the bar are waxed, cast, and welded by means of brazing.<sup>3,5,6,14,22</sup> Although it has been used for many years, this is a

technique that requires a longer working time, has a higher cost of materials, and is not effective in joining titanium or its alloys.<sup>1,3</sup> More precise and simpler techniques can be used to achieve these goals. Thus, besides the use of prefabricated bars,<sup>1,2,4</sup> which need not be cast, different types of welding — such as laser<sup>2-4,5,7,8,10-12,14,22</sup> and arc welding, TIG (Tungsten Inert Gas) or plasma<sup>1-4,6,7,8,9,11,17,16</sup> — have been studied over the past 40 years.

TIG welding is a technique whereby the highly localized heating of metal is done by means of a plasma arc established between the non-consumable electrode and the workpiece to be welded, leading to melting of the base metal,<sup>2-4,6,7,9,11,14,16,17,19,20</sup> generating welded joints with good quality and finish.<sup>2,3</sup> Furthermore, this technique allows for the welding of many alloys, including titanium alloys, since the welding is done with protective gas such as helium and argon or a mixture thereof.<sup>2-4,6,7,9,11,14,16,17,19,20</sup>

In this scenario, titanium alloys are the most used for study, including studies targeted at prosthetic frameworks, because they have the advantages of good compatibility, low density, and anti-corrosion properties.<sup>1-5,7-9,11,13,15,17-19,21</sup> However, there is great difficulty in casting and welding these alloys because, with high temperatures, they show high reactivity with oxygen, nitrogen and hydrogen, causing them to become contaminated and leaving the welded regions of the framework more vulnerable.<sup>1-9,12,13,15,17-19</sup> Thus, the TIG welding technique is well-suited for titanium and its alloys.

Regarding the method of evaluation, much research has been directed to the application of nondestructive methods — such as evaluation by liquid penetrant,<sup>4</sup> radiographic inspection,<sup>1,4,11,17</sup> micro-CT,<sup>18,21</sup> and finite element modeling — added to the destructive tests<sup>1,4,11,17</sup> for a better understanding of these regions.

The purpose of this study was to evaluate the mechanical behavior of the Ti-6Al-4V alloy with different diameters subjected to the TIG welding technique by application of the ultimate tensile strength (UTS) test, Vickers Hardness test, and the Finite Element Method (FEM). The hypotheses tested were that: (1) there would be no difference between the control and welded groups in terms of UTS and Elongation Percentage (EP); (2) increasing the diameters would not

influence the parameters (UTS, welded area percentage [WAP], and EP); and (3) there would be a difference in hardness values for the different regions - Base Metal (BM), Heat-affected Zone (HAZ), and Welded Zone (WZ).

## **MATERIAL AND METHODS**

### ***Ultimate Tensile Strength (UTS), Elongation Percentage (EP), and Welded Area Percentage (WAP)***

Forty-five dumbbell-shaped rods were machined from Ti-6Al-4V alloy (Realum; Indústria e Comércio de Metais Puros e Ligas Ltda) based on the ASTM E 8 norm<sup>25</sup> with 2.5-, 3-, 4-, and 5-mm diameters in the central segment and 84-mm length with 35-mm useful length. The specimen size was obtained from a calculation in the SigmaPlot program, with a .95 power of analysis. The specimens were machined into halves to be welded later in the TIG machine (NTY 60C; Kernit) (n=10); those belonging to the control group (CG) were machined intact (n=5). The specimens were divided into 5 groups: CG, TIG2.5, TIG3, TIG4, and TIG5.

The specimen halves were aligned in the metal matrix so that the parts to be welded were in complete abutment, to allow for standardization of the welding position for all groups. The TIG machine was adjusted for working with a 60-Å depth (current density) and 120-ms pulse (continuous arc), and the welding was performed by the same operator (M.B. Santos) at one sitting. For this technique, 2 opposite welding points were marked to stabilize the specimens. The framework was then removed from the matrix to facilitate the welding of the entire circumference.<sup>2</sup>

After the welding procedures, the welded regions were evaluated radiographically (Timex 70; Gnatus) by digital imaging (X-Scan Duo; Air Techniques) for the detection of any defects, represented by radiolucent points at the joints.<sup>1,4,15,17</sup> Additionally, a dye-revealing liquid (VP 30; Metal- Chek) was applied for the detection of any surface failure.<sup>4</sup>

The UTS measurement was carried out in a universal testing machine (MTS 810; Material Test System Corp) at a crosshead speed of .02 mm/min and 2500-Kgf load cell. The UTS (MPa) was recorded when the specimens fractured, and the EP was obtained by subtraction of the final length from the initial length, with the result divided by the initial length. The initial length was obtained after welding was completed and was measured with a digital caliper. The final length was measured by positioning of the correct halves of the specimens fractured after UTS testing in the metal matrix so that fractures remained juxtaposed; this was also measured with a digital caliper. Percentages were obtained when the differences were multiplied by 100.<sup>2</sup>

After the UTS test, both parts of the fractured specimens were subjected to evaluation of welding penetration in the fractured region through photographs taken by a digital camera, with the distance standardized and calibrated with macro increase and automatic function standardized and calibrated with the welded areas. The captured images were analyzed with Motic Images Plus 2.0 software for Windows (Motic; Richmond). All areas (mm<sup>2</sup>) were measured and tabulated. The average for each specimen and then the average for all specimens were calculated. The values obtained were converted to percentages so that the different diameters could be compared.<sup>2</sup>

### ***Scanning Electron Microscopy (SEM)***

Since the specimens in each group had similar fracture patterns, 3 specimens of each diameter were subjected to SEM at ×20, ×100, ×500, and ×1000 magnification, and those images that were most representative were used to demonstrate the welded penetration area and the failure characteristics (JSM 5600LV; JEOL).

### ***Vickers Hardness***

Samples were subjected to the Vickers hardness test at a microhardness equipment (Shimadzu), according to ASTM E92 for measurement of hardness

in different sections of the specimen – BM, HAZ, and WZ. Ten pyramidal impressions were obtained in each section of the test piece for subsequent statistical analysis.

### ***Finite Element Analysis (FEM)***

Three-dimensional FE models based on the original 3.0-mm specimens used in the experimental analysis (UTS) were constructed by computer-aided design (CAD) software (Solidworks; Dassault Systems) for both intact and welded specimens.<sup>2</sup> The welded specimens were divided into 5 different parts: the region of the dumbbell, the region of the useful length without the weld region, the welded zone, the heat-affected zone, and the region of internal void. All parts were considered completely joined except the region of the internal void. The models of intact and welded specimens were then transferred to FE processing software (Abaqus 6.12; Dessault Systèmes).

To ensure consistency and accuracy in the simulations for this study, all FE models had a mesh with quadratic tetrahedral elements of C3D10 type, with high element density in the welded region of the specimen. The 3D models contained a total of 15229 elements and 23812 nodes for nonwelded specimens and 22369 elements and 36014 nodes for welded specimens.

All materials were assumed to behave with linear elasticity. The mechanical properties of the base material were 113.8 GPa and 0.342 for Young's modulus and Poisson's ratio, respectively<sup>26</sup>. The Young's modulus increased an estimated 20% for the WZ and 10% for the HAZ, because hardness increased at these percentages in these regions, based on the values of the Vickers test. Boundary conditions were defined in constraints on displacement and rotation in all direction of both sides of the specimens, allowing movement only in the X axis. The loading configuration followed that of the UTS analysis, with its direction parallel to the X axis. The load values used were obtained from the UTS test. After the processing step, data were obtained on displacement on the X axis (mm) and on maximum principal stress (MPa), and stress x strain curve were plotted.

Model validation was performed for the intact specimen. The values of the load applied in the UTS intact specimens were used as a reference for computer simulation. Strain and stress values of the numerical models were then compared with the results of the experimental group. Stress x strain curves were close, so the FE model was validated.<sup>2</sup>

### ***Statistical Analysis***

In the initial analysis, the goal was to determine the influence of one factor involved in this study: diameter. Therefore, the data were analyzed with 1-way ANOVA, and the Dunnett test was used to evaluate the differences in UTS and EP of the control and the 4 experimental groups. The Tukey test was also used to compare test groups in all parameters analyzed: UTS, EP, and WAP. The UTS and EP values were transformed into square root. After this, the Pearson correlation test was performed to correlate UTS with WAP.

The data were also analyzed with 1-way ANOVA to evaluate the differences in the factor 'Vickers hardness' in different regions of the specimen (BM, HAZ, and WZ). The Tukey test was also used to compare the regional values. For all tests, groups were considered statistically different at  $\alpha=.05$ .

The data found in the FE analysis were analyzed by direct comparative models generated for welding processes in relation to the model generated for the intact specimen and between the experimental and numerical models. At this time, in the FEM, the term 'experimental' was used to designate specimens that were subjected to the UTS test, whether or not they were welded.<sup>2</sup>

## **RESULTS**

### ***Ultimate Tensile Strength (UTS), Elongation Percentage (EP), Welded Area Percentage (WAP), and Vickers Hardness (VH)***

Mean and standard deviation values for the UTS (MPa) in each tested group, without and with the control group, are shown in Tables I and II,

respectively. The 1-way ANOVA showed significant differences among the groups for UTS values ( $df=3$ ,  $F=88.93$ ,  $P<.001$ ) (Table III). The Dunnett test showed that the tested groups TIG3, TIG4, and TIG5 had UTS values lower than those of the control group, but the tested group TIG2.5 was not statistically significantly different in relation to control (Table II). The Tukey test showed that the UTS values of the specimens with 2.5-mm diameter were significantly higher than those of the specimens with 3.0-mm ( $P<.001$ ), 4.0-mm ( $P<.001$ ), and 5.0-mm diameters ( $P<.001$ ), the UTS values of the specimens with 3.0-mm diameter were significantly higher than those of the specimens with 4.0-mm ( $P<.001$ ) and 5.0-mm diameters ( $P<.001$ ), and the UTS values of the specimens with 4.0- and 5.0-mm diameter were not significantly different ( $P=.984$ ).

Mean and standard deviation values for the WAP (%) in each tested group are shown in Table I. The 1-way ANOVA showed significant differences among the groups for WAP values ( $df=3$ ,  $F=50.32$ ,  $P<.001$ ) (Table IV). The WAP values of the specimens with 2.5-mm diameter were significantly higher than those of specimens with 3.0-, 4.0-, and 5.0-mm diameters ( $P<.001$ ), the values for specimens with 3.0-mm diameter were also significantly higher than those of specimens with 5.0-mm diameter ( $P=.049$ ) but not significantly different from those of specimens with 4.0-mm diameter ( $P=.093$ ), and the specimens with 4.0- and 5.0-mm diameters were not significantly different ( $P=.991$ ). Pearson correlation tests showed a positive (.913) correlation between UTS and WAP.

Mean and standard deviation values for the EP (%) in each tested group without and with the control group are shown in Tables I and II, respectively. For EP values, the 1-way ANOVA showed significant differences among the groups ( $df=3$ ,  $F=13.78$ ,  $P<.001$ ) (Table V). The Dunnett test showed that all tested groups had lower EP values than the control group. The Tukey test showed that the EP values of the specimens with 2.5-mm diameter were significantly higher than those of specimens with 3.0-, 4.0-, and 5.0-mm diameter ( $P<.001$ ).

**Table I.** Means  $\pm$  standard deviations (SD) for ultimate tensile strength (MPa), welded area (%), and elongation (%), and statistical categories defined by Tukey test

<b>Diameter</b>	<b>Ultimate Tensile Strength (MPa)</b>	<b>Welded Area Percentage (%)</b>	<b>Elongation Percentage (%)</b>
	<b>Mean <math>\pm</math>SD</b>	<b>Mean <math>\pm</math>SD</b>	<b>Mean <math>\pm</math>SD</b>
2.5	990.72 $\pm$ 130.47 <sup>A</sup>	87.65 $\pm$ 16.36 <sup>A</sup>	1.39 $\pm$ . 75 <sup>A</sup>
3.0	640.77 $\pm$ 86.97 <sup>B</sup>	49.22 $\pm$ 5.96 <sup>B</sup>	.35 $\pm$ .09 <sup>B</sup>
4.0	400.98 $\pm$ 75.52 <sup>C</sup>	37.67 $\pm$ 8.91 <sup>BC</sup>	.32 $\pm$ .16 <sup>B</sup>
5.0	381.20 $\pm$ 78.43 <sup>C</sup>	36.27 $\pm$ 8.68 <sup>C</sup>	.39 $\pm$ .27 <sup>B</sup>

Different capital letters represent significant difference identified by Tukey HSD test for welding type in each parameter ( $P < .05$ ). Different lowercase letters represent significant difference identified by Tukey HSD test for diameters of specimen in each weld and each parameter.

**Table II.** Mean fracture resistance values (N) and standard deviations (SD), ultimate tensile strength (MPa) and elongation values (%) of control and experimental groups (n=5), and  $P$  values calculated by Dunnett test

	<b>Ultimate Tensile Strength</b>	<b><math>P</math></b>	<b>Elongation</b>	<b><math>P</math></b>
<b>Group</b>	<b>(MPa)</b>		<b>Percentage (%)</b>	
CG	1008.5 $\pm$ 37.1 <sup>a</sup>	-	7.5 $\pm$ 1.2 <sup>a</sup>	-
TIG2.5	990.72 $\pm$ 130.47 <sup>a</sup>	=.984	1.39 $\pm$ . 75 <sup>b</sup>	<.001
TIG3.0	640.77 $\pm$ 86.97 <sup>b</sup>	<.001	.35 $\pm$ .09 <sup>b</sup>	<.001
TIG4.0	400.98 $\pm$ 75.52 <sup>b</sup>	<.001	.32 $\pm$ .16 <sup>b</sup>	<.001
TIG5.0	381.20 $\pm$ 78.43 <sup>b</sup>	<.001	.39 $\pm$ .27 <sup>b</sup>	<.001

\*Data were analyzed by 1-way ANOVA and Dunnett test ( $\alpha = .05$ ).



**Table III.** One-way ANOVA (1×4) for ultimate tensile strength values (MPa) of welded groups

Source of Variation	Df	Sum of Square	Mean Square	F	P
Between Groups	3	937.531	312.510	88.931	<.001
Residual	36	126.507	3.514		
Total	39	1064.039			

**Table IV.** One-way ANOVA (1×4) for welded area values (%) of welded groups

Source of Variation	Df	Sum of Square	Mean Square	F	P
Between Groups	3	17292	5764	50.328	<.001
Residual	36	4123	114		
Total	39	21416			

**Table V.** One-way ANOVA (1×4) for elongation values (%) of welded groups

Source of Variation	Df	Sum of Square	Mean Square	F	P
Between Groups	3	11.365	3.788	13.784	<.001
Residual	36	9.894	.275		
Total	39	21.259			

Mean and standard deviation values for Vickers hardness in each area are shown in Table VI. The 1-way ANOVA showed significant differences among the regions (df=2, F=129.966,  $P<.001$ ) (Table VII). The Tukey test showed that the WZ values were significantly higher than those for HAZ and BM ( $P<.001$ ), and those for HAZ were higher than those for BM ( $P<.001$ ).

**Table VI.** Means  $\pm$  standard deviations (SD) for Vickers hardness

Region	Vickers Hardness (MPa)	<i>P</i>
	Mean $\pm$ SD	
Base Metal	334.29 $\pm$ 8.79 <sup>A</sup>	<.001
HAZ	365.14 $\pm$ 7.82 <sup>B</sup>	<.001
Welded Region	393.193 $\pm$ 8.17 <sup>C</sup>	<.001

Different capital letters represent significant difference identified by Tukey HSD test for welding type in each parameter ( $P < .05$ ).

**Table VII.** One-way ANOVA for Vickers hardness in different regions

Source of Variation	Df	Sum of Square	Mean Square	F	<i>P</i>
Between Regions	2	17782	8891	129.966	<.001
Residual	27	1847	68		
Total	29	19630			

### ***Scanning Electron Microscopy (SEM)***

Figures 1 and 2 are SEM images (original magnification  $\times 100$  and  $\times 20$ , respectively) of the fractured welded area of TIG3 specimens. Figure 1 shows that the fracture in Ti-6Al-4V material after TIG welding presents a fairly flat overall surface with shallow dimples, indicating a small amount of ductility. Figure 2 shows that a major portion of the central area was not joined and the presence of many voids and porosities in the welded area.

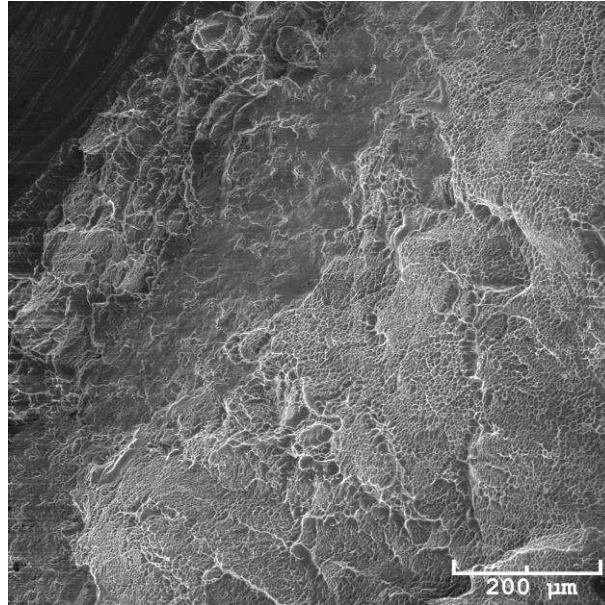


**Figure 1.** Scanning electron microscope images of specimen from the TIG3 group at ×100 magnification.

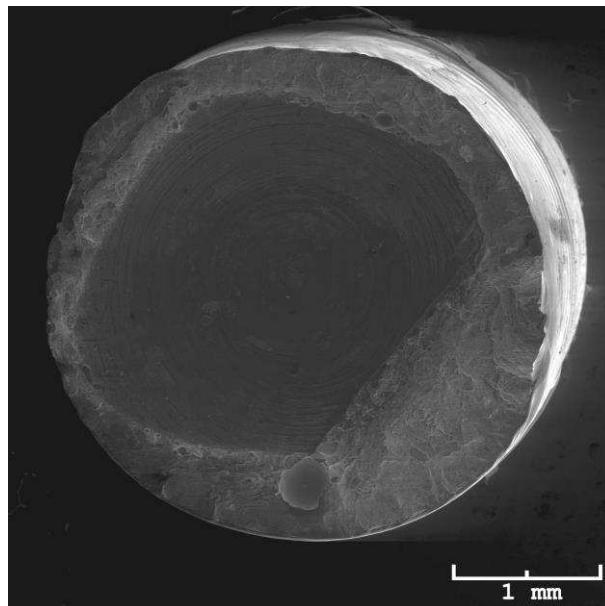


**Figure 2.** Scanning electron microscope images of specimen from the TIG3 group at ×20 magnification.

### ***Finite Element Analysis***

The values obtained from the FE models were compared with the values from the experimental models for directional deformation on the X axis, strain and stress for both intact and TIG-welded specimens for selected loads applied.

The stress x strain graph (Figure 3) shows that the curves for the experimental and FE model were very close. It could be seen that the stress concentration was throughout the central body of the intact specimen, meaning that fracture can occur at any point in this region; otherwise the welded sample has a higher concentration of stresses in the welded joint (Figure 4 and 5), mainly in the nonwelded region (Figure 6).

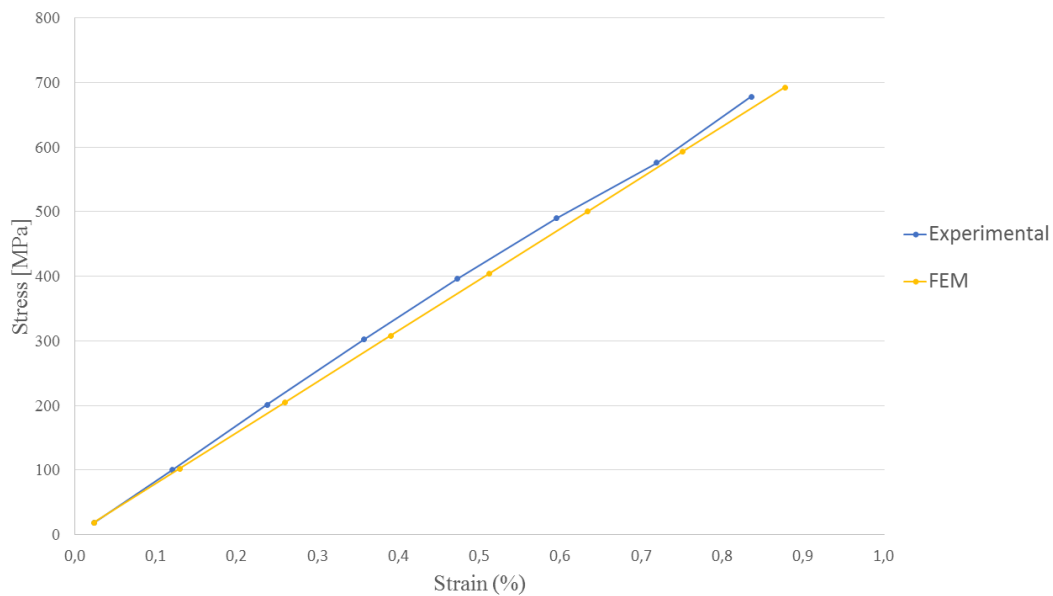


**Figure 3.** Stress x strain curve of welded specimen.

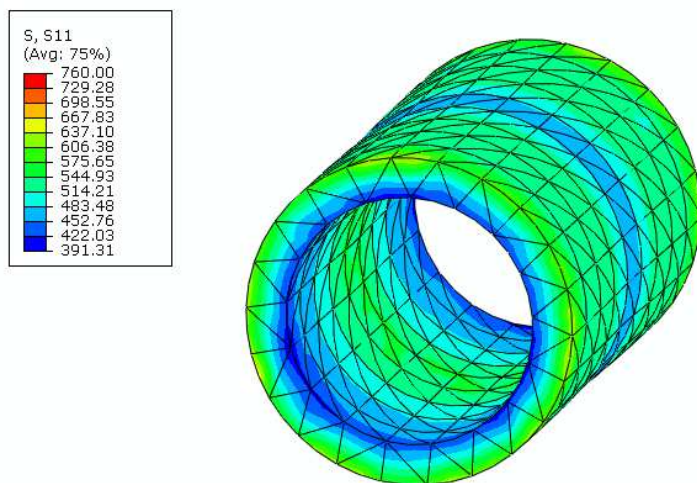


**Figure 4.** Model showing stress concentrations throughout welded metal.

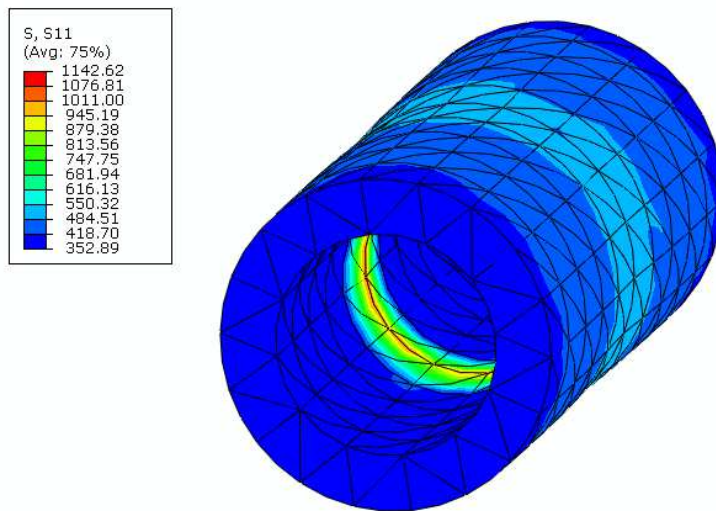


**Figure 5.** Model showing stress concentrations throughout HAZ zone.

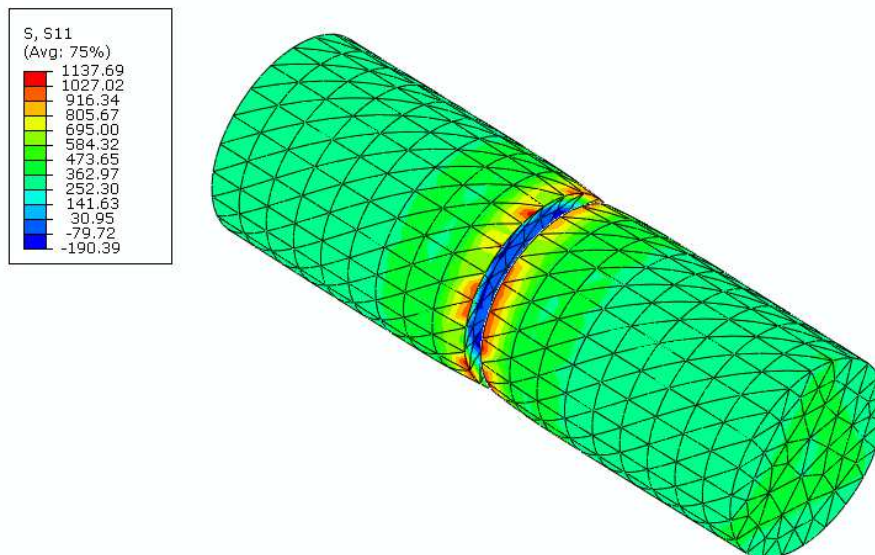


**Figure 6.** Model showing stress concentrations throughout nonwelded metal with an internal void.

## DISCUSSION

The first hypothesis of this study was partially rejected. The 1-way ANOVA showed significant differences among the groups for UTS values ( $P < .001$ ) and for EP values ( $P < .001$ ). For UTS, the Dunnett test showed that

the tested groups TIG3, TIG4, and TIG5 had values lower than those of the control group, but tested group TIG2.5 had no statistically significant difference in relation to control. For EP, the Dunnett test showed that all tested groups had values lower than those of the control group.

Under suitable welding conditions, the resistance of welded joints should correspond to the resistance of specimens not welded.<sup>2,5,7-9,14</sup> Thus, fracture can occur in any region of the cross-section of the sample<sup>2,5,7,8,11</sup> and not necessarily in the welded region<sup>2</sup>.

This behavior was identified only in the TIG2.5 group, where six of the 10 samples fractured in the base metal and not in the welded joint. In the other groups, all fractures occurred in the welded joint showing characteristics compatible with a ductile fracture on SEM images and the fractured samples in the welded area showed brittle fracture characteristics in some areas and ductile fracture in others, in addition to having a large internal void (Figures 1 and 2), confining the weld to only the periphery of the sample.<sup>1-4,7,9,22</sup> This characterization of the fractures in welded samples also explains why the elongation values were lower for them than for intact samples, since welding reduces the ductility of titanium.<sup>2,5</sup> Thus, the second hypothesis of this work was also rejected. The Tukey test showed that the values of the 2.5-mm-diameter specimen were significantly higher than those for specimens with 3.0-, 4.0-, 5.0-mm diameter ( $P<.001$ ) for all parameters analyzed (UTS, WAP, and EP).

The occurrence of a large internal void caused by incomplete penetration could be one of the most significant factors for joint weakening.<sup>1-8,15,17,19,22,24</sup> Several factors may contribute to this incomplete penetration, such as: changes in mechanical, physical, and chemical properties of metal resulting from the cooling and solidification of the metal after welding<sup>2,19,23</sup>; the regulation of the welding machine parameters<sup>1,8,10,12,13,17,21</sup>; and the configuration of the joints.<sup>4,17,18,21,24</sup>

Among the parameters that can be adjusted are: peak power (current density or electrical voltage),<sup>8,10,13</sup> pulse duration,<sup>1,8,10,13,21</sup> and the diameter of the spot weld.<sup>10,13,21</sup> Among these factors, variations in peak power appear to be the factor that most influences weld penetration.<sup>8</sup> In this work, the same

current of 60A and the same pulse of 120 ms were used, especially in the large-diameter samples with incomplete penetration, confirmed by 1-way ANOVA, which showed significant differences among the groups for WAP values ( $df=3$ ,  $F=50.32$ ,  $P<.001$ ).

In relation to joint configuration, some authors have claimed that I-shaped joints confine the welder only to the periphery of the sample, thereby generating a large internal void.<sup>2-4,17,22</sup> In all samples of the G3, G4, and G5 groups, the weld was confined to the periphery of the sample because of the joint configuration (Figure 2). Other joint configurations could be used, such as the X-shape, which favors greater weld penetration.<sup>4,17</sup> Simamoto et al.<sup>4</sup> proposed the use of welded joints in the X-shape, and the mechanical behavior of the welded joints was greatly improved. TIG welding associated with the X-shaped design resulted in higher joint resistance, similar to that of the control group.

Moreover, in the SEM image, it was possible to detect bubbles or porosities inside the weld (Figure 2). It is possible that the porosities and internal voids are a result of the inclusion of the shielding gas (argon or helium) used in the TIG welding technique and necessary to maintain an inert atmosphere during the welding procedure and minimize interaction with the oxygen, hydrogen and nitrogen from the air.<sup>2-4,13,15,17</sup>

Internal voids in the form of bubbles act as both initiators and shortcomings of fracture, since they concentrate stress and can lead to the failure of welded structures in a short period of time under the application of stresses below those that an appropriately welded joint can bear.<sup>2-4,17</sup> The finite element models showed that there was a higher concentration of stresses in the welded joints (Figures 4 and 5), most likely because of internal voids (Figure 6).

Two other factors could have influenced these results: the ability of the welder and the sharpening of the tungsten electrode. Some authors<sup>18,20,21,24</sup> allege that different welders and welder experience can also influence weld quality, but in this present work a single experienced welder welded all samples at one sitting, and therefore it is possible that the effects of this variable were minimized. Regarding sharpening, if a good-quality welded joint can be

achieved, the non-consumable tungsten electrode requires sharpening in accordance with the specifications of the equipment manufacturer for each new spot weld.<sup>2-4</sup> Since that was achieved in this work, it is likely that this variable had no influence on the results.

Finally, the third hypothesis of this work was accepted. The 1-way ANOVA showed significant differences among the regions ( $df=2$ ,  $F=129.966$ ,  $P<.001$ ) (Table VII). The Tukey test showed that values for the WZ were significantly higher than those for the HAZ and BM ( $P<.001$ ), and that those for HAZ were higher than those for BM ( $P<.001$ ). These differences among regions are a result of microstructural changes of the material after being welded.<sup>6,7,13</sup> However, resistance, in this case, depended primarily on the flaws (bubbles and internal porosities) more than on the metal properties in WZ.<sup>5</sup>

Suggestions for future studies include fatigue tests, micro-CT evaluation, metallography, and residual contraction evaluation. Additionally, although the Ti-6Al-4V alloy was used in this work because of its favorable chemical, mechanical, and biological properties, other alloys can be used for evaluation and compared with the results obtained in this work.

## CONCLUSIONS

Within the limitations of this research, the diameters of 2.5 and 3.0 mm showed the highest values of UTS and WAP and seem to be the best option for joining prefabricated bars for use in prosthetic frameworks for TIG welding, in terms of machine regulation and configuration of the joints used in this study.

## REFERENCES

1. Lyra e Silva JP, Fernandes Neto AJ, Raposo LH, Novais VR, de Araujo CA, Cavalcante L de A, et al. Effect of plasma welding parameters on the flexural strength of Ti-6Al-4V alloy. *Braz Dent J* 2012;23:686-91.
2. Castro MG, Araújo CA, Menegaz GL, Silva JPL, Nóbilo MAA, Simamoto-Júnior PC. Laser and Plasma dental soldering techniques applied to Ti-6Al-4V alloy: Ultimate tensile strength and finite element analysis. *J Prosthet Dent* 2015;113:460-4663.



3. Silveira-Júnior CD, Castro MG, Davi LR, Neves FD, Novais VR, Simamoto-Júnior PC. Welding techniques in dentistry. In: Kovacevic R, editor. *Welding Processes*. 17<sup>th</sup> ed. Croatia: In tech;2012, p.415-38.
4. Simamoto-Júnior PC, Novais VR, Machado AR, Soares CJ, Raposo LHA. Effect of joint design and welding type on the flexural strength and weld penetration of Ti-6Al-4V alloy bars. *J Prosthet Dent* 2015; 113:467-474.
5. Berg E, Wagnere WC, Davik G, Dootz ER. Mechanical properties of laser-welded cast and wrought titanium. *J Prosthet Dent* 1995;74:250-7.
6. Wang RR, Welsch GE. Joining titanium materials with tungsten inert gas welding, laser welding, and infrared brazing. *J Prosthet Dent* 1995;74:521-30.
7. Neo TK, Chai J, Gilbert JL, Wozniak WT, Engelman MJ. Mechanical properties of titanium connectors. *Int J Prosthodont* 1996; 9(4):379-93.
8. Chai T, Chou CK. Mechanical properties of laser-welded cast titanium joints under different conditions. *J Prosthet Dent* 1998;79:477-83.
9. Taylor JC, Hondrum SO, Prasad A, Brodersen CA. Effects of joint configuration for the arc welding of cast Ti-6Al-4V alloy rods in argon. *J Prosthet Dent* 1998;79:291-7.
10. Baba N, Watanabe I. Penetration depth into dental casting alloys by Nd:YAG laser. *J Biomed Mater Res B Appl Biomater* 2005;72:64-8.
11. Rocha R, Pinheiro AL, Villaverde AB. Flexural strength of pure Ti, Ni-Cr and Co-Cr alloys submitted to Nd:YAG laser or TIG welding. *Braz Dent J* 2006;17:20-3.
12. Watanabe I, Topham DS. Laser welding of cast titanium and dental alloys using argon shielding. *J Prosthodont* 2006;15:102-7.
13. Akman E, Demir A, Canel T, Sinmazçelik T. Laser welding of Ti6Al4V titanium alloy. *J Mater Proc Technol* 2009;209:3705-13.
14. Byrne G. Soldering in prosthodontics - an overview, part I. *J Prosthodont* 2011;20:233-43.
15. Nuñez-Pantoja JM, Takahashi JM, Nóbilo MA, Consani RL, Mesquita MF. Radiographic inspection of porosity in Ti-6Al-4V laser-welded joints. *Braz Oral Res* 2011;25:103-8.

16. Barbi FC, Camarini ET, Silva RS, Endo EH, Pereira JR. Comparative analysis of different joining techniques to improve the passive fit of cobalt-chromium superstructures. *J Prosthet Dent* 2012; 108:377-85.
17. Nunez-Pantoja JM, Farina AP, Vaz LG, Consani RL, Nóbilo MA, Mesquita MF. Fatigue strength: effect of welding type and joint design executed in Ti-6Al-4V structures. *Gerodontology* 2012; 29:1005-10.
18. Takayama Y, Nomoto R, Nakajima H, Ohkubo C. Effectes of argon flow rate on laser-welding. *Dent Mater J* 2012; 31(2):316-326.
19. Atoui JA, Felipucci DNB, Pagnano VO, Orsi IA, Nóbilo MAA, Bezzon L. Tensile and flexural strength of commercially pure titanium submitted to laser and tugsten inert gas welds. *Braz Dent J* 2013; 24(6):630-634.
20. Castro GC, Araújo CA, Mesquita MF, Consani RLX, Nóbilo MAA. Stress distribution in Co-Cr implant frameworks after laser or TIG welding. *Braz Dent J* 2013; 24(2):147-151.
21. Ghadhanfari HÁ, Hasan MK, Monaco EA, Hyeongil K. Effectes of soldering methods on tensile strength of gold-palladium metal ceramic alloy. *J Prosthet Dent* 2014; 112:994-1000.
22. Takayama Y, Nomoto R, Nakajima H, Ohkubo. Comparasion of joint designs for laser welding of cast metal plates and wrought wires. *Odontology* 2013; 101:34-42.
23. Bertrand C and Poulon-Quintin. Temporal pulse shaping: a key parameter for the laser welding of dental alloys. *Laser Med Sci* 2015; 30:1457-1464.
24. Kokolis J, Chakmakchi M, Theocharopoulos A, Prombonas A, Zinelis S. Mechanical and interfacial characyerization of laser welded Co-Cr alloy with diferente joint configurations. *J Av Prosthodont* 2015; 7:39-46.
25. American Society for Testing and Materials International. Designation: E 8M – 04: Standard Test Methods for Tension Testing of Metallic Materials [Metric]. West Conshohocken: ASTM; 2004. 24 p.
26. Materials Properties Handbook: Titanium alloys materials properties handbook. Editores: Gerhard Welsch, Rodney Boyer, E.W. Collings. Editora: ASM International, 1993. 1176 pág.

### **3.3. Evaluation of X-shaped welded joints with Co-Cr alloy under different welding parameters: analysis by micro-CT and flexural strength**

Morgana G. Castro, DDS, MSc<sup>a</sup>; Leandro M. S. Resende, DDS<sup>b</sup>; Átila P. Teles, DDS, MSc, PhD<sup>c</sup>; Ricardo T. Lopes, DDS, MSc, PhD<sup>d</sup>; Paulo César Simamoto Júnior, DDS, MSc, PhD<sup>e</sup>

#### **ABSTRACT**

Statement of the problem. The literature provides limited information regarding the parameters and performance of Co-Cr TIG joints welded in prefabricated bars in dental applications. Purpose. The purpose of this study was to evaluate the mechanical strength correlated to the percentage of the total volume of weld and porosities of Co-Cr alloy joints welded with TIG technique. Material and methods. Thirty Co-Cr alloy bar specimens were perpendicularly sectioned to the long-axis and rejoined by using X30-shaped joint design with TIG welding. Then they were divided into 3 groups (n=10): the CG1 with a 60-A depth (current density) and 90-ms pulse (continuous arc); the CG2 with a 60-A depth and 120-ms pulse and the CG3 with a 60-A depth and 160-ms pulse. The specimens were submitted to nondestructive tests: radiographic inspection, penetrant liquid and Micro-CT (to calculate the percentage of the total volume of welding and the porosities) and then tested with 3-point bending. The fracture surfaces were analyzed with scanning electron microscopy (SEM). The data were statistically analyzed with 1-way ANOVA and the Tukey *post hoc* test for all the variables which were analyzed: flexural strength, total volume of weld and porosities. Pearson correlation test was also applied ( $\alpha=.05$  for all statistical tests). Results. The 1-way ANOVA showed that the factors machine parameters were not significant for flexural strength values ( $P=.231$ ), the total volume of weld ( $P=.057$ ) and porosities ( $P=.057$ ). There are no significant relationships between any pair of variables

after Pearson correlation test ( $P > .050$ ). Conclusions. Under the experimental conditions described, there was no statistical difference in the groups suggesting that the three machine regulation can be an option for joining prefabricated Co-Cr rods in this kind of union.

Keywords: Dental Alloys; Dental Soldering; Micro- CT, Flexural strength.

**CLINICAL IMPLICATIONS:** Co-Cr prefabricated bars and the TIG (Tungsten Inert Gas) welding technique are less time-consuming and costly than the conventional technique and may be used to make implant frameworks for patients with an edentulous maxilla or mandible.

## INTRODUCTION

Implantology focused on the oral rehabilitation of edentulous patients has been well-documented and extensively performed, with high success rates.<sup>1,2</sup> This rehabilitation model, which became known *ad modum* as the Brånemark Protocol, has been the subject of several studies, both in relation to implants and with respect to the metallic framework.<sup>1-24</sup>

The studies focused on prosthetic frameworks were developed to optimize their production by the use of prefabricated bars and welding techniques other than conventional welding.<sup>1-24</sup> Studies have been conducted to evaluate the types of welding techniques,<sup>1,2,4,7,8,10,14,15,18,19,23,24</sup> the settings of welding equipment,<sup>1,5,7,11</sup> the types of alloys used,<sup>1,8,9,17,20,23</sup> the settings of the joints,<sup>10,15,17,22,24</sup> and mechanical methods of evaluation of these weld joints.<sup>2,13,17,20</sup>

Among the welding techniques, two have been identified for dental use: laser welding<sup>2-5,7-11,12-20,22,23</sup> and TIG or plasma welding.<sup>1,2,4,6,8,12,14-16,18,19,23,24</sup> Both have some advantages: welding can be performed directly on the model,<sup>2,5,7,8,10,14,16</sup> energy can be concentrated in a small area,<sup>1,2,8,14,16,20</sup> resulting in a reduced HAZ (Heat affected zone)<sup>2,7,13,16</sup> although laser welding has an even smaller HAZ than TIG welding,<sup>2,18</sup> allowing for repair in regions close to the resin and ceramic<sup>2,5,8-10,13,15,16,22</sup>), good finish weld pool, the

possibility for welding in any position,<sup>2,16</sup> and less time required compared with that needed for conventional welding.<sup>2,7,8,10,16,22</sup> The decision regarding how a welding technique will be used should be based on the availability of equipment.<sup>14</sup> However, the cost of equipment is markedly different between techniques, with the laser welding equipment being much more expensive than the TIG equipment and often unavailable for use by the prosthesis-manufacturing laboratories.<sup>2,16,18</sup>

Regardless of the technique used, studies have shown that the welding machine configuration appears to exert influence on the welding process. Studies have been developed to investigate the influence of parameters such as: current density or electric voltage (peak power),<sup>5,7,11</sup> pulse duration,<sup>1,5,7,11,20</sup> the diameter of the spot weld,<sup>7,11,20</sup> and the use of the argon shield<sup>9,11,17</sup> in penetration depth.

Akman et al.<sup>11</sup> studied the effects of different parameters on the laser welding of Ti-6Al-4V specimens in relation to penetration depth and concluded that peak power was the most important parameter, but if that power was increased too much, the temperature of the workpiece exceeded the evaporation point of the alloy and promoted crater formation on the surface of the material. To increase penetration depth without craters, pulse duration was increased and thus the width of the heat-affected zone, the weld pool, was increased at the same penetration depth.

The type of alloy has also been studied.<sup>1,8,9,17,20</sup> While titanium alloys are most often used in studies because of their advantages of good compatibility, low density, and anti-corrosion properties,<sup>1-3,5,6,8,11,13,16-18,20,24</sup> casting and welding these alloys can be difficult, since titanium, when subjected to high temperatures, has high oxygen, nitrogen, and hydrogen reactivity and can become contaminated, leaving the welded areas of the framework more vulnerable.<sup>1-6,9,11,13,15-18,24</sup> Moreover, Co-Cr alloys are increasingly popular in prosthetic dentistry, due to a favorable combination of biocompatibility, resistance to corrosion, castability, weight, stiffness, and low cost.<sup>8,10,14,22</sup>

The configuration of the joint is another factor influencing the resistance of welded joints.<sup>2,13,15,20,22,24</sup> Castro et al.<sup>2</sup> evaluated the mechanical strength of

Ti-6Al-4V alloy frameworks with samples of different diameters with an I-shaped joint configuration welded with both laser and plasma techniques. They found that there was incomplete penetration in all samples and that the internal void left thereby may have been one of the main reasons for the decreased strength in the welded joints. Similar results were found by Zupanic et al.<sup>10</sup> and Kokolis et al.<sup>21</sup> in I-shaped joints of Co-Cr subjected to laser welding.

Simamoto et al.<sup>23</sup> proposed the use of welded joints in X-shaped frameworks, which greatly improved their mechanical behavior. TIG welding associated with the X-shaped design resulted in higher joint resistance, similar to that of the control group. Furthermore, in the same study, they evaluated two different angles of this type of chamfer and concluded that an X-shaped design with a 60-degree chamfer had better strength values than designs with a 45-degree chamfer. Contrary results were found by Zupanic et al.<sup>10</sup> in laser-welded Co-Cr samples in which the change in the configuration of the joint to an X-shape did not increase resistance values.

Finally, in joint evaluations, investigators have been increasingly attempting to understand the mechanical behavior of welded frameworks and propose improvements in welding processes. Therefore, most studies have used non-destructive tests such as radiographic evaluation<sup>1,8,13,15,24</sup> as well as destructive tests with the ultimate tensile test<sup>2-6,9-11,17,18,20</sup> and bending test.<sup>1,8,18,24</sup> However, few studies have used tests such as evaluation by micro-CT<sup>17,20</sup> and evaluation by the finite element method.<sup>2</sup> Among these, micro-CT facilitates the 3-dimensional evaluation of all welded inner areas, allowing for the identification and calculation of porosities and internal voids<sup>17,20</sup> and for the evaluation and calculation of solder volume in the joint.

The purpose of this study was evaluation of the mechanical strength of a Co-Cr alloy in different machine regulations of the TIG technique by the application of micro-CT (for calculation of the percentage of the total volume of weld and porosities) and the 3-point bending test. Two hypotheses were tested: the first, that differences would be found between the machine regulations in relation to flexural strength and total volume of weld but not in relation to porosities; and the second, that there would be positive correlation between the

flexural strength and total volume of weld and between the flexural strength and porosities for all groups.

## MATERIAL AND METHODS

Thirty Co-Cr alloy bar specimens were sectioned perpendicular to the long axis and re-joined in an X30-shaped joint design (3.18 mm in diameter × 40.0 mm in length) (Figure 1) with TIG welding and divided into 3 groups (n=10): CG1, with a 60-Å depth (current density) and 90-ms pulse (continuous arc); CG2, with a 60-Å depth and 120-ms pulse; and CG3, with a 60-Å depth and 160-ms pulse. For construction of the specimen design, segments were milled at their extremities with a lathe (PRN-320; IMOR), producing 1-mm-deep X-shaped chamfers with 30-degree angles between the bar extremities.<sup>10,15,24</sup>

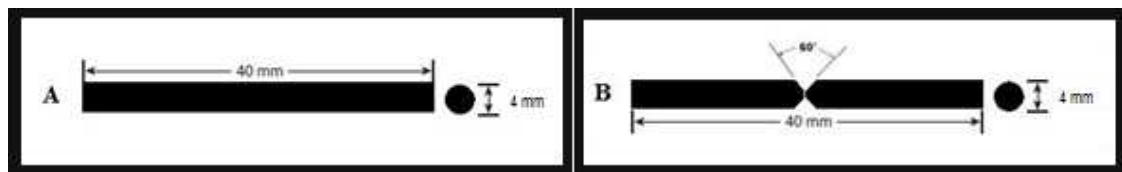


**Figure 1.** Geometry of specimens in X-shaped joint design with 30-degree chamfer.

For standardization, the specimens were fixed in a holding matrix to ensure that both halves were properly aligned and juxtaposed during welding procedures.<sup>1,24</sup> TIG welding was performed with specific dental equipment (NTY60C; Kernit) set to 60-Å depth and pulse range according to group. The electrode was placed perpendicular to the segment to be welded at a .5-mm distance, as recommended by the manufacturer. Two opposite welding points were initially made, connecting the central part of the joint and stabilizing the specimens. The framework was then removed from the matrix to facilitate the welding of the entire circumference.<sup>2</sup> After every 2 welds, the electrode was cleaned to ensure adequate performance. The argon gas flow rate was set to 10 L/min, and the flow began 2 seconds before and ended 2 seconds after the welding procedure to allow the specimens to cool in an inert atmosphere.<sup>24</sup> TIG welding was performed by the same operator (L.R. Miranda).

After the welding procedures, the welded regions were evaluated radiographically (Timex 70; Gnatus) by digital imaging (X-Scan Duo; Air Techniques) for the detection of defects, represented by radiolucent points at the joints. Additionally, a dye-revealing liquid (VP 30; Metal-Chek) was applied for the detection of surface failure.<sup>13,24</sup> Specimens that showed failure were discarded and replaced.

The welded areas of all specimens were observed by means of a micro-CT device (SkyScan1173, Bruker micro-CT NV Belgium). The tube voltage was 130 kV for the Co–Cr alloy; the current produced by the X-ray generator was 61 Å. X-ray image acquisition was performed with a CCD camera equipped with the micro-CT device. In total, 517 slices of the welded areas of the specimens were obtained vertically along the lengths of the specimens. The thickness of each slice was .016 mm. These images were reconstructed by cross-section images from tomography projection images (SkyScan NRecon; Bruker micro-CT NV Belgium), and then 3-dimensional models were constructed with the use of image analysis software (CT-Analyser [CTAn]; Bruker micro-CT NV Belgium). The sizes, numbers, and total volume ratios of welding and the bubbles and spaces present in the specimens were also determined with the software. The percentage of total welding volume was calculated based on the entire welded area, including the bubbles and spaces. The percentage of porosities was calculated from the total volume ratios of the bubbles and the spaces.<sup>17</sup>

Specimens were tested for flexural strength in 3-point bending design with 3-mm-diameter rods and 20-mm span-length between supports. Compressive loading was applied at .5 mm/min crosshead speed with a 3-mm-diameter rod positioned at the center of the specimen. The test was considered finished when any sudden loading change (load drop) representing failure or permanent deformation of the beam was detected, until a maximum displacement of 5 mm. The flexural strength (MPa) of the specimens was obtained according to the following equation:  $fs = 8FL/\pi D^3$ , where fs is the flexural strength (MPa), F is the value of fracture strength or elastic limit (N), L is the distance between supports, and D is the diameter of the specimen (mm).<sup>1,24</sup>



Since the specimens in each group had similar fracture patterns, 3 specimens of each group were subjected to SEM at  $\times 20$ ,  $\times 50$ ,  $\times 100$ ,  $\times 200$ , and  $\times 500$  magnification, and those images that were most representative were used to demonstrate the failure pattern characteristics (JSM 5600LV; JEOL).

The data were statistically analyzed, separately, with 1-way ANOVA and the Tukey post hoc test for all variables analyzed: flexural strength and total volume of weld and porosities. The Pearson correlation test was used to correlate the flexural strength and total volume of weld and to correlate the flexural strength and porosities for all groups ( $\alpha=.05$  for all statistical tests).

## RESULTS

Mean and standard deviation values for flexural strength (MPa) in each tested group are shown in Table 1. The 1-way ANOVA showed that machine regulation factors ( $P=.231$ ) were not significant for flexural strength values (Table 2).

Mean and standard deviation values for the total volume of weld (%) in each tested group are shown in Table 1. For total volume of weld, the machine regulation factors ( $P=.287$ ) were not significant (Table 3).

Mean and standard deviation values for porosity (%) in each tested group are shown in Table 1. For porosity, the machine regulation factors ( $P=.289$ ) were not significant (Table 4).

**Table I.** Mean and standard deviations (SD) for Flexural strength (MPa), total volume of weld (%) and porosities (%), and statistical categories defined by Tukey test.

Groups	Flexural Strength (MPa) Mean $\pm$ SD	Total volume of weld (%) Mean $\pm$ SD	Porosities (%) Mean $\pm$ SD
CG1	1536.2 $\pm$ 278.9 <sup>A</sup>	99.7 $\pm$ 0.1 <sup>A</sup>	0.3 $\pm$ 0.1 <sup>A</sup>
CG2	1679.8 $\pm$ 235.7 <sup>A</sup>	99.6 $\pm$ 0.2 <sup>A</sup>	0.4 $\pm$ 0.2 <sup>A</sup>
CG3	1507.5 $\pm$ 177.9 <sup>A</sup>	99.3 $\pm$ 0.7 <sup>A</sup>	0.7 $\pm$ 0.7 <sup>A</sup>

Different capital letters represent significant difference identified by Tukey HSD test for different groups in each parameter ( $P<.05$ ).

**Table II.** One-way ANOVA for flexural strength values (MPa) of groups

Source of variation	Df	Sum of Square	Mean square	F	P
Between groups	2	170439	85219	1.550	.231
Residual	27	1484829	54993		
Total	29	1655269			

**Table III.** One-way ANOVA for total volume of weld values (%) of groups

Source of variation	Df	Sum of square	Mean square	F	P
Between groups	2	.185	.0924	1.306	.287
Residual	27	1.911	.0708		
Total	29	2.096			

**Table IV.** One-way ANOVA for porosities values (%) of groups

Source of variation	Df	Sum of square	Mean square	F	P
Between groups	2	.184	.0921	1.300	.289
Residual	27	1.913	.0709		
Total	29	2.097			

Figures 2 and 3 are micro-CT images of the welded area, and Figures 4 and 5 are SEM images of the fractured welded area. Figures 2 and 3 show the total volume of the welded area and the porosities (bubbles and spaces) inside the welded area. Figures 4 and 5 show the failure pattern characteristics. Figure 4 shows partial fracture in the welded region, and Figure 5 presents a fairly flat overall surface with shallow dimples, indicating ductility of the fracture.

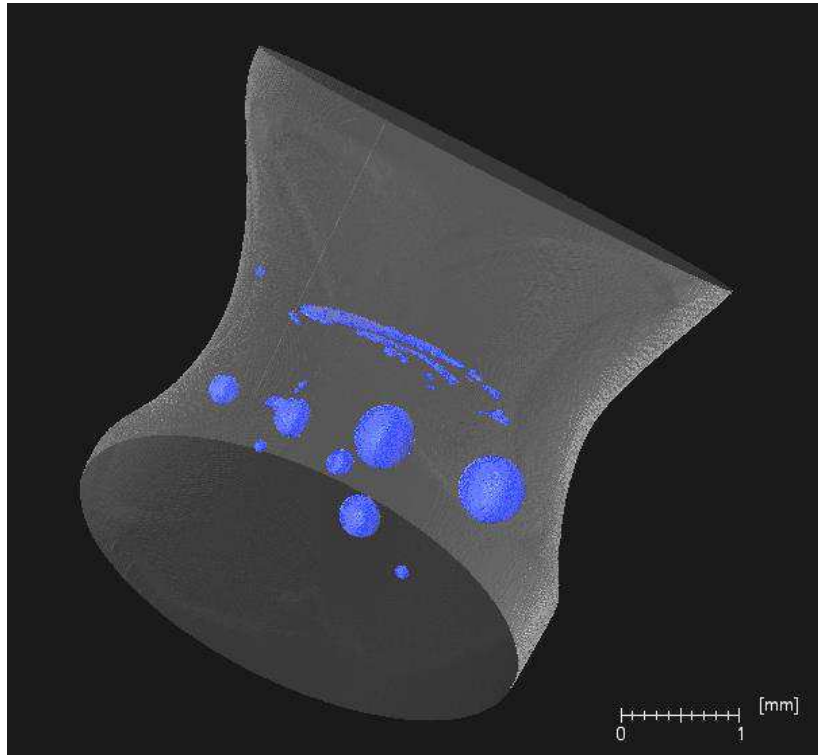


**Figure 2.** Micro-CT image of specimen from CG1.

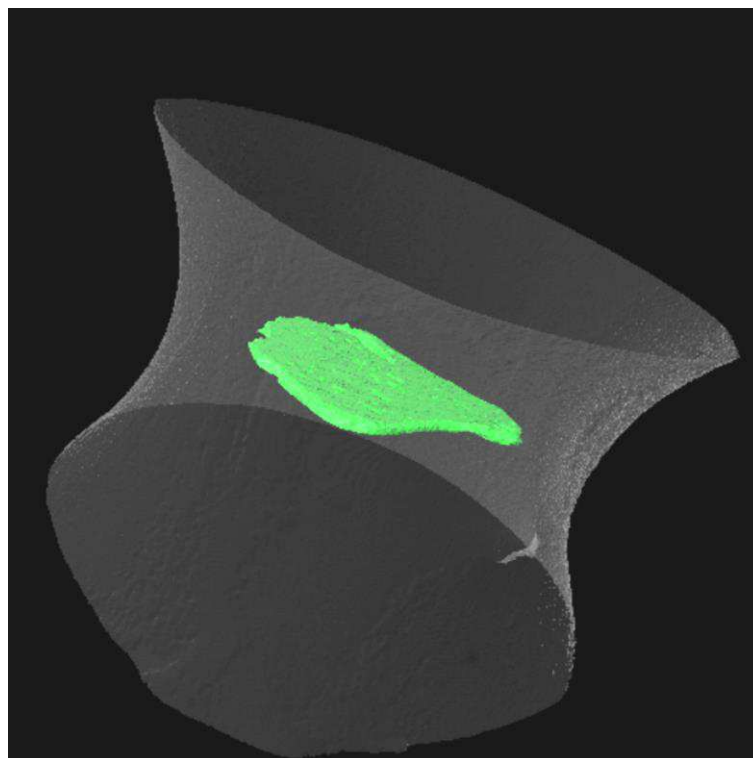


**Figure 3.** Micro-CT image of specimen from CG2.

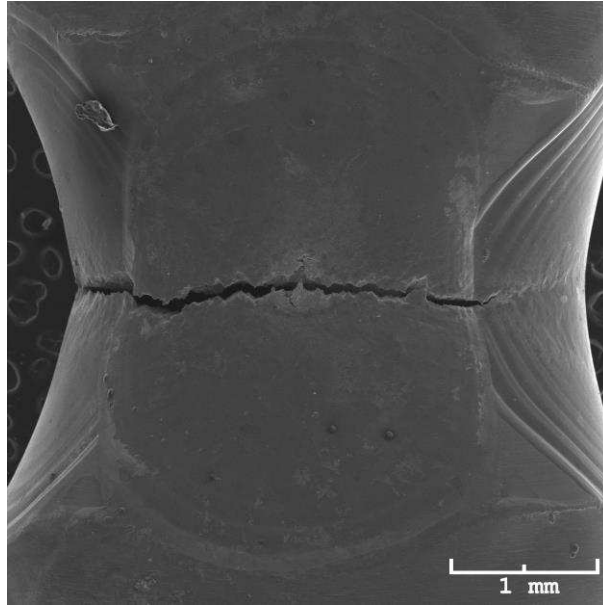


**Figure 4.** Scanning electron microscope images at  $\times 20$  magnification of specimen from CG3.

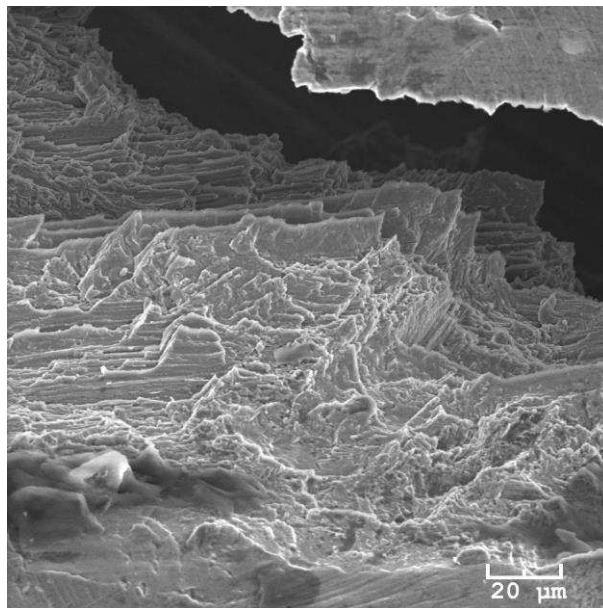


**Figure 5.** Scanning electron microscope images at  $\times 500$  magnification of specimen from CG2.

## DISCUSSION

The first hypothesis tested — that differences would be found between the machine regulation in relation to flexural strength and total volume of weld

but not in relation to porosities — was partially rejected. The 1-way ANOVA showed that machine regulation factors ( $P=.231$ ) were not significant for flexural strength values, for total volume of weld, and for porosity ( $P=.289$ ).

Several factors could account for this result, such as welding technique,<sup>1-5,7-11,14-17,20,23,24</sup> the variations in the welding parameters of the equipment used,<sup>1,5,7,9,11,17,20</sup> the presence of porosities and internal voids,<sup>1-5,9,10,13,15,17,20,22,24</sup> welder experience,<sup>17,19,20,22</sup> and the correct sharpening of the tungsten electrode.<sup>2,24</sup>

In TIG welding, the heating of metal is too highly localized by a plasma arc established between the non-consumable electrode and the workpiece to be welded, leading to melting of the base metal,<sup>1,2,4,6,8,14-16,18,19,24</sup> generating welded joints with good finish (mainly in small-diameter structures<sup>2,16</sup>), and therefore, since the samples were of the same diameter (3.18 mm), metal fusion was similar in all groups, which was confirmed by micro-CT images (e.g. Figures 1 and 2) showing similar weld volumes in the different samples of different groups. Further, the measurement of the weld volume showed no statistically significant difference between groups ( $P=.287$ ) (Table 1).

Under optimal welding conditions, the resistance of welded joints should be equivalent to that of unwelded samples<sup>2,3,5,6</sup>; however, incomplete penetration could generate internal porosities and voids that could be significant weakening factors.<sup>1-5,10,13,15,18,22,24</sup> This incomplete penetration may result from several factors, such as: the cooling and solidification of the metal after being welded<sup>20</sup>, altering the mechanical, physical, and chemical properties of metal<sup>2,18</sup>; vaporization of volatile alloying elements<sup>15</sup>; or regulation of the welding machine parameters.<sup>1,5,7,9,11,15,20</sup> Among the parameters that can be adjusted are current density or electric voltage (peak power),<sup>5,7,11</sup> pulse duration,<sup>1,5,7,11,20</sup> the diameter of the spot weld,<sup>7,11,20</sup> and the use of an argon shield.<sup>9,11,17</sup>

Chai and Chou<sup>5</sup> evaluated the mechanical properties of commercially pure Ti subjected to laser welding under different conditions to determine the best welding parameters relative to voltage and pulse duration. They found that there was no statistically significant difference in the pulse duration factors for

UTS values and concluded that voltage was the only factor that affected the resistance values of welded samples. Baba and Watanabe<sup>7</sup> examined the penetration depth into different casting alloys under several laser welding conditions. They concluded that when the voltage increased and the spot diameter decreased, the penetration depth increased for each metal. Similar values were found by Lyra e Silva et al.<sup>1</sup>, who reported that the variations in pulse duration on the plasma welding machine showed no statistically significant difference when the same current was maintained for samples of Ti-6Al-4V in the flexural strength test.

Therefore, since, in the present study, the same current of 60 Å was used and only the pulse duration varied (90, 120, and 160 ms), the results are similar to those obtained in the aforementioned studies. The 1-way ANOVA showed that machine regulation factors ( $P=.231$ ) were not significant for flexural strength values.

Moreover, it is possible that, in this study, the porosities and internal voids were also the result of inclusion of the shielding gas (argon or helium) used in the TIG welding technique<sup>2,11,13,15,16,24</sup> and/or incomplete weld penetration, also caused by the shielding gas.<sup>9</sup> Although in this work an X-shaped joint was used, which favors greater weld penetration,<sup>15,24</sup> different from that of I-shaped joints that confine welding to only the periphery of the sample, generating a large internal void,<sup>2,10,15,24</sup> it can be detected on the micro-CT images (e.g. Figures 2 and 3) that all samples had porosities and internal voids and all fractured in the welded region (Figure 4). Watanabe and Thopam<sup>9</sup> investigated the effect of argon shielding gas on the resistance of laser-welded joints in different alloys, among them the Co-Cr alloy, and concluded that, at a constant current of 220 V and a pulse duration of 10 ms, the samples welded without the shielding gas showed resistance values higher than those of samples welded in the presence of gas. This is because the oxidation of Co-Cr is limited to the sample surface, favoring the penetration of the weld into the interior of the alloy. Takayama et al.<sup>17</sup> used micro-CT to evaluate the porosities of laser-welded Co-Cr samples with different flow rates of protective gas and found that the greater the amount of gas, the higher the number of porosities.

Therefore, it is likely that porosities and internal voids were the result of the inclusion of the shielding gas and incomplete weld penetration caused by the gas itself. These porosities and internal voids acted as stress concentration points and led the structures to fail in the welded region during destructive tests.<sup>2,4,5,15,24</sup>

Thus, in ideal situations, welded areas should behave as do base metals,<sup>2,3,5,6</sup> and breakage could occur, or not, in any region of the cross-section,<sup>2,3,5,8</sup> or there would be only metal plastic deformation, because of the type of mechanical test used in this study – 3-point bend test with a 5-mm deformation limit and collapse of 20%. However, all samples broke at the welding joint, which led to the conclusion that these porosities actually led to the failure of the welded joint.<sup>2,3,5,10,15,24</sup>

Moreover, the fact that the second hypothesis of this work was rejected (there were no significant relationships between pairs of variables after the Pearson correlation test [ $P > .050$ ]) leads to two conclusions: The first, given independent quantitative differences or sizes of porosities and internal voids, means that the simple fact of the existence of a porosity indicates stress concentration at this point, with crack propagation leading to failure in these regions.<sup>2,10,15,16,24</sup> The second is that the weld volume had no positive correlation with resistance values and possibly a larger volume of solder in all specimens would not change this statistical results. This conclusion has been reached since, in this work, welded metal was not added, causing a constriction in the welded region (Figures 2, 3, and 4), although the TIG welding technique permits its use.<sup>15,16,23,24</sup>

Regarding the welder, some authors<sup>17,19,20,22</sup> claimed that different welders and their levels of experience can also influence the weld quality, but in this present work a single experienced welder welded all samples at one sitting, and therefore it is possible that the effects of this variable were minimized. Regarding the sharpening of the electrode, the tungsten electrode should be kept sharpened, in accordance with the manufacturer's specifications, before each new spot weld to improve the quality of the welded joint.<sup>2,24</sup> Since this was

achieved in this work, it is likely that this variable had no influence on the results.

Moreover, there are limitations to the longevity of these structures; therefore, aging tests such as corrosion behavior<sup>10,23</sup> and fatigue tests<sup>15</sup> should be conducted to assess this condition. In addition, studies in which these structures were applied to the cylinder fabricating the bars for clinical use are necessary to evaluate longevity in relation to the cylinder in a complete framework.<sup>10</sup> Further studies in relation to masticatory forces exerted by patients on these structures are also necessary to establish benchmarks for comparison with the values obtained in this and other studies.

In addition to the future work already mentioned above, other studies should be developed with the same methodologies to evaluate not only welding processes but also casting processes, with other metal alloys and with different diameters.

## **CONCLUSIONS**

Within the limitations of this research and after the finding that the machine parameter is only one aspect to be considered in evaluation of the success of welding techniques, the three different machine parameters used in this work can be regarded as options for joining prefabricated bars in prosthetic frameworks by TIG welding in terms of the configuration of the joints used in this study.

## **REFERENCES**

1. Lyra e Silva JP, Fernandes Neto AJ, Raposo LH, Novais VR, de Araujo CA, Cavalcante L de A, et al. Effect of plasma welding parameters on the flexural strength of Ti-6Al-4V alloy. *Braz Dent J* 2012;23:686-91.
2. Castro MG, Araújo CA, Menegaz GL, Silva JPL, Nóbilo MAA, Simamoto-Júnior PC. Laser and Plasma dental soldering techniques applied to Ti-6Al-4V



alloy: Ultimate tensile strength and finite element analysis. J Prosthet Dent 2015;113:460-4663.

3. Berg E, Wagnere WC, Davik G, Dootz ER. Mechanical properties of laser-welded cast and wrought titanium. J Prosthet Dent 1995;74:250-7.

4. Wang RR, Welsch GE. Joining titanium materials with tungsten inert gas welding, laser welding, and infrared brazing. J Prosthet Dent 1995;74:521-30.

5. Chai T, Chou CK. Mechanical properties of laser-welded cast titanium joints under different conditions. J Prosthet Dent 1998;79:477-83.

6. Taylor JC, Hondrum SO, Prasad A, Brodersen CA. Effects of joint configuration for the arc welding of cast Ti-6Al-4V alloy rods in argon. J Prosthet Dent 1998;79:291-7.

7. Baba N, Watanabe I. Penetration depth into dental casting alloys by Nd:YAG laser. J Biomed Mater Res B Appl Biomater 2005;72:64-8.

8. Rocha R, Pinheiro AL, Villaverde AB. Flexural strength of pure Ti, Ni-Cr and Co-Cr alloys submitted to Nd:YAG laser or TIG welding. Braz Dent J 2006;17:20-3.

9. Watanabe I, Topham DS. Laser welding of cast titanium and dental alloys using argon shielding. J Prosthodont 2006;15:102-7.

10. Zupancic R, Legat A, Funduk N. Tensile strength and corrosion resistance of brazed and laser-welded cobalt-chromium alloy joints. J Prosthet Dent 2006;96:273-82.

11. Akman E, Demir A, Canel T, Sinmazçelik T. Laser welding of Ti6Al4V titanium alloy. J Mater Proc Technol 2009;209:3705-13.

12. Byrne G. Soldering in prosthodontics - an overview, part I. J Prosthodont 2011;20:233-43.

13. Nuñez-Pantoja JM, Takahashi JM, Nóbilo MA, Consani RL, Mesquita MF. Radiographic inspection of porosity in Ti-6Al-4V laser-welded joints. Braz Oral Res 2011;25:103-8.

14. Barbi FC, Camarini ET, Silva RS, Endo EH, Pereira JR. Comparative analysis of different joining techniques to improve the passive fit of cobalt-chromium superstructures. J Prosthet Dent 2012; 108:377-85.

15. Nunez-Pantoja JM, Farina AP, Vaz LG, Consani RL, Nóbilo MA, Mesquita MF. Fatigue strength: effect of welding type and joint design executed in Ti-6Al-4V structures. *Gerodontology* 2012; 29:1005-10.
16. Silveira-Júnior CD, Castro MG, Davi LR, Neves FD, Novais VR, Simamoto-Júnior PC. Welding techniques in dentistry. In: Kovacevic R, editor. *Welding Processes*. 17<sup>th</sup> ed. Croatia: In tech;2012, p.415-38.
17. Takayama Y, Nomoto R, Nakajima H, Ohkubo C. Effectes of argon flow rate on laser-welding. *Dent Mater J* 2012; 31(2):316-326.
18. Atoui JA, Felipucci DNB, Pagnano VO, Orsi IA, Nóbilo MAA, Bezzon L. Tensile and flexural strength of commercially pure titanium submitted to laser and tugsten inert gas welds. *Braz Dent J* 2013; 24(6):630-634.
19. Castro GC, Araújo CA, Mesquita MF, Consani RLX, Nóbilo MAA. Stress distribution in Co-Cr implant frameworks after laser or TIG welding. *Braz Dent J* 2013; 24(2):147-151.
20. Takayama Y, Nomoto R, Nakajima H, Ohkubo. Comparasion of joint designs for laser welding of cast metal plates and wrought wires. *Odontology* 2013; 101:34-42.
20. Bertrand C and Poulon-Quintin. Temporal pulse shaping: a key parameter for the laser welding of dental alloys. *Laser Med Sci* 2015; 30:1457-1464.
21. Kokolis J, Chakmakchi M, Theocharopoulos A, Prombonas A, Zinelis S. Mechanical and interfacial characyerization of laser welded Co-Cr alloy with diferente joint configurations. *J Av Prosthodont* 2015; 7:39-46.
22. Matos IC, Bastos IN, Diniz, MG, Miranda MS. Corrosion in artificial saliva of a Ni-Cr-based dental alloy joined by TIG welding and conventional brazing. *J Prosthet Dent* 2015; 11:278-285.
23. Simamoto-Júnior PC, Novais VR, Machado AR, Soares CJ, Raposo LHA. Effect of joint design and welding type on the flexural strength and wel penetration of Ti-6Al-4V alloy bars. *J Prosthet Dent* 2015; 113:467-474.

### **3.4. Maximum bite force measurement in patients subjected to different rehabilitation treatments – a pilot study**

Morgana Guilherme de Castro<sup>a</sup>; Brunna Alves Paes Leme<sup>b</sup>; Isabella Cristina Rodrigues Tavares<sup>c</sup>; Veridiana Resende Novais<sup>d</sup>; Paulo César Simamoto Júnior<sup>e</sup>

#### **Summary**

Background: Maximum bite force (MBF) is an indicator related to the functional state of the stomatognathic apparatus and influences both muscle development and masticatory function. Objective: the objective of this work was to evaluate two different types of prosthetic rehabilitation and compare their values in individuals with normal occlusion and without any prosthetic rehabilitation. Method: Thirty-six patients were divided into 3 groups: a control group (CG) (n = 14), consisting of completely dentate patients with bilateral occlusion and simultaneous and well-distributed contacts; a PTP group (n = 12), consisting of patients with dentures and three mandibular implants; and a PT group (n = 10), consisting of patients with bimaxillary dentures. To obtain MBF records, gnathodynamometry was used for measurement of both sides, and the sum of the two sides was used as the total value of the individual's MBF. Result: there was no statistically significant difference between genders for MBF in both experimental groups, but there was a statistically significant difference for the type of treatment, with the total MBF in the CG being higher than that in the other groups, followed by the PTP group and finally the PT group. Conclusion: it was concluded that implant prostheses increased the maximum bite force in edentulous patients and that gender did not influence any of the groups analysed.

Keywords: complete denture, bite force, implant-supported prosthesis, bite force recording devices, mastication, implants.

## Background

Maximum bite force (MBF) is an indicator related to the stomatognathic apparatus and influences both muscle development and masticatory function (1-3); thus, it can be used as a method to evaluate the function, activity and efficiency of the jaw muscles (1,3-5) and as a parameter of normality (2). However, many variations have been reported for this parameter from studies conducted in different populations and with different individual factors as well as with different techniques and measurement devices (1,3-7).

The individual factors are related to morphological, physiological and biomechanical craniofacial variables (1,7), such as type of occlusion (1), facial morphology (1,7), body mass index (1), functional disorders of the stomatognathic apparatus, the position of the head at the time of the measurement (1,5), dentition status (4,5), the strength of the jaw muscles at closing, the pain threshold of the subject, age (1,4), and gender (1,2,8). Bite force also varies according to the region in the mouth and is highest in the first molar region (3,4). Thus, most of the works using the first molar region for the measurement of maximum bite force (1,3,7,8).

Furthermore, the type of treatment also influences the MBF (3,6-10). In edentulous patients treated with bimaxillary dentures, more than 30% complained of their prostheses, especially in relation to retention, instability and pain whilst chewing, particularly with respect to mandibular prostheses (11). Users of conventional dentures have been reported to have a masticatory efficiency and a maximum bite force lower than those found for individuals with natural dentition (6,7,12,13).

Conversely, studies have shown that patients subjected to treatment with mandibular dentures supported by implants reported a significant improvement in stability, retention, masticatory function, muscles effort and improved quality of life compared with patients who were treated with conventional dentures only (6-9,14).

The measurement techniques and the mechanical characteristics of the bite force system, as stated earlier, also play an important role in the variations

found for this parameter (3,7). A wide range of devices have been used to measure maximum bite force, including: bite fork (14), strain gauge transducers (1,6,8,9,11,15), gnathodynamometer (7), blade transducers, a pressurised rubber tube, a pressure-sensitive sheet (16) and a sensor resistance force (4,10,17). Some investigators (3-5,18,19) used a device called the GM10 bite force meter (Nagano Keiki, Tokyo, Japan) to measure maximum bite force.

Therefore, the objective of this study was to measure maximum bite force (MBF) by means of a gnathodynamometer in different individuals subjected to different rehabilitation treatments (PTP group, individuals with dentures and a three-mandibular-implant protocol; PT group, individuals with bimaxillary dentures) and compare the results between groups as well as in relation to individuals with satisfactory occlusion and no rehabilitation treatment (control group), in both males and females. The hypotheses of this study were that men would have MBF values higher than those of women in all groups, that the control group would present higher values than the test groups, and that, between the test groups, MBF values for patients in the PTP group would be greater than those of patients in the PT group.

## **Materials and methods**

This cross-sectional study was ethically approved by the research committee (042022/2014) for human studies of the Federal University of Uberlândia (CEP / UFU). Participants were invited to participate after evaluation based on criteria for inclusion and exclusion. Those who agreed to participate were kept informed of how the research would be carried out and signed a free and informed consent document (ICF), which provided comprehensive information about the development of the research.

Seventy-three patients who attended the dental hospital of the Dentistry School of the Federal University of Uberlândia and were eligible to participate in this research were screened. The inclusion criteria were that participants had to: be at least 18 years old, fit into one of the proposed research groups, agree to participate in all stages of the research and sign the informed consent

document. Individuals were excluded if they: were diagnosed with temporomandibular disorder, had a systemic disease that might affect their neuromuscular system, had periodontal disease, had parafunctional habits, were under 18 years old and did not fit into one of the groups proposed for this study.

In total, 44 individuals met the inclusion criteria and were recruited into the study. Gender and type of treatment were recorded for each participant. Participants were divided into 3 groups (Table 1): a Control Group (CG), consisting of fully dentate individuals with bilateral and simultaneous occlusion with well-distributed contacts and without premature contact or occlusal interference; a PTP group, consisting of individuals with maxillary dentures and three mandibular implants; and a PT group, consisting of individuals with conventional dentures.

**Table 1.** Group distribution

Group	Number of individuals	
	Female	Male
CG	11	11
PTP	8	4
PT	6	4

#### *MBF records*

For MBF records to be obtained, each participant remained seated in a dental chair with his/her head in a comfortable position, keeping the Frankfurt plane parallel to the ground (1,3,5,16,17). A gnathodynamometer was used (Kratos industrial equipment LTDA, Cotia, SP) (Fig. 1), and the subject was instructed to bite as hard as possible for 2 or 3 s (5,9,16,20) 5 times on each side in the first molar region (1,7-10,14,17,20,21) (Fig. 1). This sequence was repeated 4 times, the first of which was used for calibration and therefore was not included in the data tabulation. A 3-minute rest time was recommended between acquisitions (15,16,21). The mean value was the MBF value on one side, and

the sum of the values of the two sides was the total value of an individual's MBF (1,17). The first molar region was chosen for measurement (7) (Fig. 2). All data acquisitions were made by the same operator.



**Fig. 1.** Gnathodynamometer.

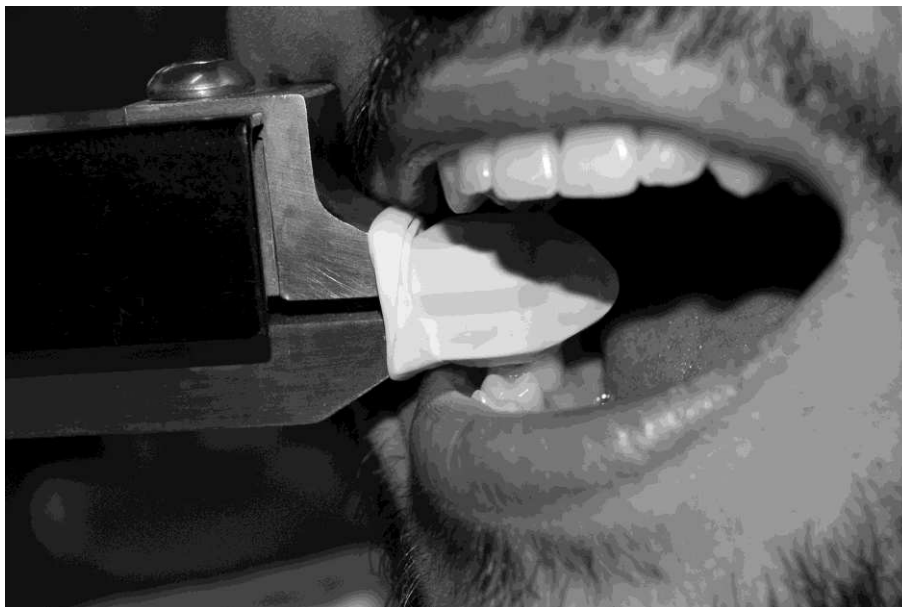


**Fig. 2.** Measurement of MBF values in the first molar region using the gnathodynamometer.

### Statistical analysis

The results were subjected to logarithmic transformation and showed normal distribution (Shapiro-Wilk). Values were then subjected to two-way ANOVA, followed by the Tukey test ( $\alpha = 0.05$ ).

### Results

The average of the right and left sides was obtained, and the sum of both sides was calculated to arrive at the total individual MMF (1,17).

The means and standard deviations of total averages of MBF values in the GC, PTP and PT groups, for both males and females, are shown in Table 2. The two-way ANOVA showed no intersections between genders ( $Df = 1$ ,  $F = 2.252$ ,  $P = 0.142$ ) and no intersections between gender and treatment type ( $Df = 2$ ,  $F = 1.390$ ,  $P = 0.261$ ), but did show intersections between types of treatment ( $Df = 2$ ,  $F = 78.294$ ,  $P < 0.001$ ).

Between types of treatment, there were statistically significant differences among all groups ( $P < 0.001$ ). The MBF values of the control group were higher than those of the test groups. Between the test groups, the MBF values of the PTP group were higher than those of the PT group.

**Table 2.** Mean and standard deviation of the MBF (N) of the groups

Type of treatment	Gender	
	Male	Female
CG	772.86 $\pm$ 213.21 <sup>Aa</sup>	516.13 $\pm$ 202.54 <sup>Aa</sup>
PTP	238.63 $\pm$ 94.50 <sup>Ab</sup>	278.25 $\pm$ 147.87 <sup>Ab</sup>
PT	100.63 $\pm$ 31.86 <sup>Ac</sup>	83.18 $\pm$ 45.40 <sup>Ac</sup>

\* Capital letters represent the comparison between genders within the same group, and lowercase letters represent the comparison between groups within the same gender. The same letters show that there was no statistically significant difference, whilst different letters show that there was.



## Discussion

The first study hypothesis was rejected. The results showed no statistically significant difference between males and females for either test group, contrary to some papers that have reported such differences, where men have higher MBF than women (1,3,8), and the authors attributed this to the male facial pattern (1,3,8), which has a higher bone arch and more muscular bone patterns (1). The masseter muscle in men has fibers with diameters larger than those in women (3). In addition, hormonal differences may contribute to the muscle fiber composition. The lower bite force in women may also be due to a lower pain threshold during the time of activation (1), or to smaller dental size, corresponding to smaller periodontal ligament areas, thus producing lower bite force values (3). However, for this study, there were no intersections between genders ( $P = 0.142$ ).

It can be seen that, although there was no statistically significant difference between genders, in the control group, the mean values for men ( $772.86 \pm 213.21$ ) were higher than those for women ( $516.13 \pm 202.54$ ). In addition, there was a large standard deviation, which demonstrated significant variation between individuals, strengthening the hypothesis that individual characteristics, population characteristics, age, race and eating habits can influence the results (1,3,4). However, as this correlation with these variables was not performed in this study, it cannot be ascertained which of these positively or negatively influenced the results.

Conversely, the second and third hypotheses of this study were accepted. The results showed that MBF values were higher in the CG, followed by the PTP and, finally, the PT. The highest values for MBF in the CG can be justified by the presence of the periodontal ligament, which provided tactile sensitivity and proprioceptive motion feedback. Gonçalves et al. (22) studied the effects of complete and partial removable dentures on chewing movements and reported that the presence of teeth and sensory input from mechanoreceptors present in the periodontal ligament of the remaining teeth play a key role in the control of jaw motion.

Similar results relative to the PTP and PT groups were found by Muller et al (12), who compared totally dentate patients, patients with bimaxillary implant-supported dentures, patients with maxillary dentures and mandibular overdentures and patients with bimaxillary dentures. The results showed that the patients with bimaxillary dentures had the lowest MBF values. Melo et al (7) evaluated patient's MBF after rehabilitation with mandibular implant-supported prosthesis correlated to facial pattern and dominant chewing side and concluded that mandibular rehabilitation with dental implants improves MBF independent of the facial pattern and dominant chewing side.

This can be explained by the fact that implant prostheses have higher mechanical retention and stability; thus, patients can develop greater strength and muscle activation, making them stronger and thereby increasing chewing force and quality of life (6,9), due to better chewing efficiency and higher MBF values (6,7,8,10).

Another point of discussion relates to the types of equipment and techniques (3). The method of acquiring maximum-strength data is important in that mechanical stimulation evokes feedback from not only excitatory but also inhibitory effects on bite force. Inhibitory effects are those assessed without damage to the teeth and other components of the stomatognathic apparatus whilst the volunteer is biting (5), with an average of 2 or 3 s (5,9,16,20) up to 7 s (10,17) reported in studies advocating a wait time between acquisitions, whilst other reports range from 2 min (20), 3 min (15,16,21) and 5 min (10) to 10 min (8).

Therefore, this study used 2 or 3 s for the acquisition of MBF values and a waiting time of 3 min. Four batteries were made with 5 acquisitions each on each side of the arch, the first of which was determined by the results from a test ascertaining that the patient understood how the equipment worked and felt safe in allowing the test to be run. The separate acquisition on each side of the arc was an attempt to reflect chewing more closely. The concomitant acquisition of the two sides greatly increased the strength in all groups.

Further studies are required on larger samples and different populations to identify the effects of age, eating habits and other physical characteristics on

the measured bite force values, in addition to evaluating other types of rehabilitation.

## **Conclusion**

Within the limitations of this study, it can be concluded that implant prostheses increased the maximum bite force in edentulous patients, although they did not attain the values found for the control group. Gender did not influence any group.

## **References**

1. Koç D, Dogan A, Bek B. Effect of gender, facial dimensions, body mass index and type of functional occlusion on bite force. *J Appl Oral Sci* 2011; 19(3):274-9.
2. Abreu RAM, Pereira MD, Furtado F, Prado GPR, Mestriner Jr W, Ferreira LM. Masticatory efficiency and bite force in individuals with normal occlusion. *Arch Oral Bio* 2014; 59(10):1065-74.
3. Al-Omiri MK, Sghaireen MG, Alhijawi MM, Alzoubi IA, Lync CD, Lynch E. Maximum bite force following unilateral implant-supported prosthetic treatment: within-subject comparison to opposite dentate side. *J Oral Rehabil* 2014; 41(8):624-9.
4. Varga S, Spalj A, Varga ML, Milosevi AS, Mestrovic S, Slaj M. Maximum voluntary molar bite force in subjects with normal occlusion. *Eur J Orthod* 2011; 33(4):427-33.
5. Serra CM & Manns AE. Bite force measurements with hard and soft bite surfaces. *J Oral Rehabil* 2013; 40(8):563-8.
6. Fontijn-Tekamp F. A., Slagter A. P., Van Der Bilt A., Van 'T Hof M. A., Witter D. J., Kalk W. and Jansen J. A. Biting and Chewing in Overdentures, Full Dentures, and Natural Dentitions. *J Dent Res* 2000; 79(7):1519-24.
7. Melo ACM, Ledra IM, Vieira RA, Coró ER, Sartori IAM. Maximum bite force of edentulous patients before and after dental implants

- rehabilitation: long-term follow-up and facial type influence. *J Prosthodont* 2016; 00:1-5 [Epub ahead of print].
8. Bilhan H, Geckili O, Mumcu E, Cilingir A, Bozdog E. The influence of implant number and attachment type on maximum bite force of mandibular overdentures: a retrospective study. *Gerodontology* 2012; 29(2):e116-20.
  9. Caloss R, Al-Arab M, Finn RA, Throckmorton GS. The effect of denture stability on bite force and muscular effort. *J Oral Rehabil* 2011; 38(6):434-9.
  10. Gonçalves T.M.S.V., Campos C.H., Gonçalves G.M., de Moraes M. and Rodrigues Garcia R.C.M. Mastication Improvement After Partial Implant-supported Prosthesis Use. *J Dent Res* 2013 92: 189S.
  11. Shah F. K., Gebreel A., Elshokouki A. H., Habib A. A., Porwal A. Comparison of immediate complete denture, tooth and implant-supported overdenture on vertical dimension and muscle activity. *J Adv Prosthodont* 2012; 4(2):61-71.
  12. Muller F, Hernandez M, Grutter L, Aracil-Kessler L, Weingart D, Schimmel M. Masseter muscle thickness, chewing efficiency and bite force in edentulous patients with fixed and removable implant-supported prostheses: a crosssectional multicenter study. *Clin Oral Implants Res* 2012, 23(2):144–150.
  13. Luraschi J, Schimmel M, Bernard JP, Gallucci GO, Belser U, Müller F.. Mechanosensation and maximum bite force in edentulous patients rehabilitated with bimaxillary implant supported fixed dental prostheses. *Clin Oral Implants Res* 2012; 23(5):577-83.
  14. Van Kampen F, Cune M, van der Bilt A, Bosman F. The effect of maximum bite force on marginal bone loss in mandibular overdenture treatment: an in vivo study. *Clin Oral Implants Res* 2005; 16(5):587-93.
  15. Geckili O, Mumcu E, Bilhan H. The effect of maximum bite force, implant number, and attachment type on marginal bone loss around implants supporting mandibular overdentures: a retrospective study. *Clinical Implant Dent Relat Res* 2012; 14(1):e91-e97.

16. Jofre J, Hamada T, Nishimura M, Klattenhoff C. The effect of maximum bite force on marginal bone loss of mini-implants supporting a mandibular overdenture: a randomized controlled trial. *Clin Oral Implants Res* 2010; 21(2):243-9.
17. Custodio W, Gomes SGF, Faot F, Garcia RCMR, Del Bel Cury AA. Occlusal force, electromyographic activity of masticatory muscles and mandibular flexure of subjects with different facial types. *J Appl Oral Sci* 2011; 19(4):343-9. Epub 2011.
18. Kamegai T, Tatsuki T, Nagano H, Mitsunashi H, Kumeta J, Tatsuki Y, Kamegai T, Inaba B. A determination of bite force in northern Japanese children. *Eur J Orthod* 2005; 27(1):53-7.
19. Owais AI, Shaweesh M, Alhaija ESJA. Maximum occlusal bite force for children in different dentition stages. *Eur J Orthod* 2013; 35(4):427-33.
20. Lepley CR, Throckmorton GS, Ceen RF, Buschang PH. Relative contributions of occlusion, maximum bite force, and chewing cycle kinematics to masticatory performance. *Am J Orthod Dentofacial Orthop* 2011; 139(5):606-13.
21. Jain V, Mathur VP, Abhishek K, Kothari M. Effect of occlusal splint therapy on maximum bite force in individuals with moderate to severe attrition of teeth. *J Prosthodont Res* 2012; 56(4):287-92.
22. Gonçalves TMSV, Vilanova LSR, Gonçalves LM, Rodrigues Garcia RCM. Effect of complete and partial removable dentures on chewing movements. *J Oral Rehabil*. 2014; 41(3):177-83.

#### 4. DISCUSSÃO GERAL

Os artigos apresentados nesta tese mostraram que vários são os fatores que influenciam os resultados quando infraestruturas metálicas são submetidas ao processo de soldagem. De maneira geral, os fatores que influenciam estes resultados podem ser categorizados em: técnica de soldagem (Berg et al., 1995; Wang and Welsh, 1995; Chai and Chou, 1998; Baba and Watanabe 2004; Watanabe and Topham, 2006; Rocha et al., 2006; Zupanic et al., 2006; Akman et al., 2008; Barbi et al., 2012; Lyra e Silva et al., 2012; Nunez-Pantoja et al., 2012; Silveira-Júnior et al., 2012; Takayama et al., 2012; Takayama et al., 2013; Castro et al., 2015; Matos et al., 2015; Simamoto Júnior et al., 2015); presença de porosidades e/ou incompleta penetração (Berg et al., 1995; Wang and Welsh, 1995; Chai e Chou, 1998; Liu et al., 2002; Watanabe and Topham, 2006; Zupanic et al., 2006; Kikuchi et al, 2011; Lyra e Silva et al., 2012; Nunez-Pantoja et al., 2011; Nunez-Pantoja et al., 2012; Takayama et al., 2012; Takayama et al., 2013; Castro et al., 2015; Kokolis et al., 2015; Simamoto-Junior et al., 2015); variação dos parâmetros de soldagem (Chai and Chou, 1998; Baba and Watanabe, 2004; Watanabe and Topham, 2006; Akman et al., 2008, Kikuchi et al., 2011; Lyra e Silva et al., 2012; Takayama et al., 2012; Takayama et al., 2013); tipos de ligas utilizados (Rocha et al 2006; Watanabe and Topham, 2006; Lyra e Silva et al., 2012; Takayama et al., 2012; Takayama et al., 2013; Matos et al., 2015); configurações das juntas soldadas (Zupanic et al., 2006; Nunez-Pantoja et al., 2012; Takayama et al., 2012; Takayama et al., 2013, Kokolis et al., 2015; Simamoto Júnior et al., 2015); métodos de avaliação mecânica dessas juntas (Nunez-Pantoja et al., 2011; Castro et al., 2015; Takayama et al., 2012; Takayama et al., 2013); experiência do operador (Takayama et al., 2012; Takayama et al., 2013; Castro et al., 2015; Simamoto Júnior et al., 2015) e correto apontamento do eletrodo de tungstênio nas técnicas TIG ou Plasma (Castro et al., 2015; Simamoto Júnior et al., 2015).

As técnicas de soldagem laser (Berg et al., 1995; Wang and Welsh, 1995; Chai and Chou, 1998; Baba and Watanabe, 2004; Watanabe and

Topham, 2006; Rocha et al., 2006; Zupanic et al., 2006; Akman et al., 2008; Nunez-Pantoja et al., 2011; Nunez-Pantoja et al., 2012; Takayama et al., 2012; Barbi et al., 2012; Atoui et al., 2013; Castro et al., 2013; Kokolis et al., 2015; Silveira-Júnior et al., 2012; Takayama et al., 2013; Castro et al., 2015) e TIG ou Plasma (Wang and Welsh, 1995; Taylor et al., 1998; Rocha et al., 2006; Lyra e Silva et al., 2012; Nunez-Pantoja et al., 2012; Silveira-Júnior et al., 2012; Barbi et al., 2012; Atoui et al., 2013; Castro et al., 2013; Castro et al., 2015; Matos et al., 2015; Simamoto Júnior et al., 2015), embora apresentem vantagens semelhantes tais como: a soldagem pode ser realizada diretamente sobre o modelo de trabalho (Chai and Chou, 1998; Baba and Watanabe, 2004; Rocha et al., 2006; Zupanic et al., 2006; Kikuchi et al., 2011; Fornaini et al., 2011; Barbi et al., 2012; Silveira-Júnior et al., 2012; Castro et al., 2015); o calor é concentrado apenas na região onde foi aplicada a fonte de energia (Rocha et al., 2006; Barbi et al., 2012; Lyra e Silva et al., 2012; Silveira-Júnior et al., 2012; Takayama et al., 2013; Castro et al., 2015), resultando em uma reduzida ZAC (Baba and Watanabe, 2004; Nunez-Pantoja et al., 2011; Silveira-Júnior et al., 2012; Castro et al., 2015), permitem o reparo das infraestruturas metálicas em regiões próximas à resina e cerâmica (Chai and Chou, 1998; Rocha et al., 2006; Watanabe and Topham, 2006; Zupanic et al., 2006; Nunez-Pantoja et al., 2011; Nunez-Pantoja et al., 2012; Silveira-Júnior et al., 2012; Castro et al., 2015; Kokolis et al., 2015); a soldagem pode ser realizada em qualquer posição (Silveira-Júnior et al., 2012; Castro et al., 2015) e necessita de menos tempo de laboratório que a soldagem convencional (Baba and Watanabe, 2005; Rocha et al., 2006; Zupanic et al., 2006; Silveira-Júnior et al., 2012; Castro et al., 2015; Kokolis et al., 2015), apresentam diferentes mecanismos de imposição de calor.

A soldagem laser é um processo de união baseado na fusão localizada da junta por meio de seu bombardeamento por um feixe de luz concentrada, coerente e monocromática de alta intensidade (Wang and Welsh, 1995; Neo et al., 1996; Fornaini et al., 2011). Uma das suas maiores vantagens é que ela produz um *Keyhole* que concentra a energia absorvida em uma pequena região, resultando em alta penetração e formação de estreita zona afetada pelo

calor (ZAC) (Chai & Chou, 1998; Liu et al., 2002; Cho et al., 2003; Rocha et al., 2006; Srimaneepong et al., 2008; Nuñez-Pantoja et al., 2011) ainda mais estreita que na soldagem TIG ou Plasma (Atoui et al., 2013; Castro et al., 2015). Já a soldagem TIG ou Plasma consiste em alto aquecimento do metal por um arco estabelecido entre o eletrodo não consumível e a peça a ser soldada (Wang and Welsh, 1995; Neo et al., 1996; Taylor et al., 1998; Rocha et al., 2006; Byrne, 2011; Barbi et al., 2012; Nunez-Pantoja et al., 2012; Silveira-júnior et al 2012; Atoui et al., 2013; Castro et al., 2013; Castro et al., 2015; Simamoto-Júnior et al., 2015), gerando juntas soldadas com bom acabamento principalmente em estruturas de pequeno diâmetro (Silveira-júnior et al., 2012; Castro et al 2015).

A decisão da técnica a ser utilizada pode ser baseada na disponibilidade do equipamento ou em preferências individuais do operador (Barbi et al., 2012). Entretanto, o custo do equipamento é uma diferença marcante entre as técnicas, em que o equipamento de solda laser é bem mais caro que o equipamento de solda TIG ou Plasma, o que muitas vezes inviabiliza o seu uso nos laboratórios de prótese (Silveira Júnior et al., 2012; Atoui et al., 2013; Castro et al., 2015).

Em relação à presença de porosidades e/ou incompleta penetração, foi possível detectar que, em todas as amostras soldadas, dos artigos apresentados nesta tese, independentemente das condições e técnicas de soldagem e independentemente das características das infraestruturas metálicas, havia a presença de porosidades e vazios internos na região da junta soldada. Em condições ideais de soldagem, a resistência das juntas soldadas deveria ser equivalente à resistência do metal base (Berg et al., 1995; Chai e Chou, 1998; Taylor et al., 1998; Liu et al., 2002; Castro et al., 2015). Entretanto, a presença dessas porosidades e/ou incompleta penetração podem ter sido um dos fatores mais significantes para a diminuição da resistência mecânica das juntas soldadas (Berg et al., 1995; Wang and Welsh, 1995; Chai e Chou, 1998; Liu et al., 2002; Zupanic et al., 2006; Kikuchi et al., 2011; Lyra e Silva et al., 2012; Nunez-Pantoja et al., 2011; Nunez-Pantoja et al., 2012; Atoui et al., 2013; Castro et al., 2015; Kokolis et al., 2015; Simamoto-Júnior et al.,



2015). Essa incompleta penetração pode ter sido causada por vários fatores, tais como: o resultado dos ciclos de resfriamento e solidificação do metal após o processo de soldagem que leva à mudanças nas propriedades mecânicas, físicas e químicas dos metais (Atoui et al., 2013; Castro et al., 2015), a volatilização de elementos da liga (Nunez-Pantoja et al., 2012) ou a regulação dos parâmetros de solda (Chai and Chou, 1998; Baba and Watanabe, 2004; Watanabe and Topham, 2006; Akman et al., 2008, Kikuchi et al., 2011; Nunez-Pantoja et al., 2012; Lyra e Silva et al., 2012; Takayama et al., 2013). Além disso, é possível que as porosidades observadas sejam resultado da inclusão do gás de proteção argônio necessário para manter uma atmosfera inerte durante os procedimentos de soldagem (Akman et al., 2008; Nunez-Pantoja et al., 2011; Nunez-Pantoja et al., 2012; Silveira Júnior et al., 2012; Castro et al., 2015; Simamoto junior et al., 2015). Tanto as porosidades quanto a incompleta penetração atuam como pontos de concentração de tensão agindo como iniciadores das fraturas nas regiões soldadas (Nunez-Pantoja et al., 2012; Silveira-Júnior et al., 2012; Castro et al., 2015; Simamoto-Júnior et al., 2015).

Em relação à variação dos parâmetros de soldagem, estudos têm sido desenvolvidos no intuito de investigar a influência de parâmetros tais como: corrente e voltagem (Chai and Chou, 1998; Baba and Watanabe, 2004, Akman et al., 2008, Kikuchi et al., 2011), duração do pulso (Chai and Chou, 1998; Baba and Watanabe, 2004; Akman et al., 2008, Kikuchi et al., 2011; Lyra e Silva et al., 2012; Takayama et al., 2013) e, diâmetro do ponto de solda (Baba and Watanabe, 2004; Akman et al., 2008, Kikuchi et al., 2011; Takayama et al., 2013). Dentre os fatores avaliados, a variação da corrente ou voltagem, parece ser o fator que mais influencia a penetração da solda (Chai and Chou, 1998). Em apenas um artigo apresentado nesta tese os parâmetros de solda variaram. Entretanto, o parâmetro variado foi a duração do pulso e esse não teve nenhuma influência nos valores de resistência nem na quantidade de porosidades e vazios internos.

No que concerne aos tipos de ligas utilizados, o titânio e suas ligas são os mais utilizados nos estudos, incluindo aqueles voltados às infraestruturas protéticas em virtude das suas vantagens tais como: boa compatibilidade, baixa

densidade e propriedades anti-corrosivas (Berg et al., 1995; Chai and Chou 1998; Neo et al., 1996; Taylor et al., 1998; Rocha et al., 2006; Akman et al., 2008; Lyra e Silva et al., 2012; Nunez-Pantoja et al., 2011; Nunez-Pantoja et al., 2012; Silveira-Júnior et al., 2012; Takayama et al., 2012, Atoui et al., 2013; Takayama et al., 2013; Castro et al., 2015; Simamoto-Júnior et al., 2015). No entanto, há uma grande dificuldade nos processos de fundição e soldagem do titânio e suas ligas, pois quando aquecido a altas temperaturas o titânio possui uma grande afinidade pelos elementos do ar (oxigênio, nitrogênio e hidrogênio), o que o torna contaminado por esses elementos, tornando as regiões das juntas soldadas mais vulneráveis (Berg et al., 1995; Wang and Welsh, 1995; Neo et al., 1996; Chai and Chou, 1998; Taylor et al., 1998; Watanabe and Tophan, 2006; Akman et al., 2008; Lyra e Silva et al., 2012; Nunez-Pantoja et al., 2011; Nunez-Pantoja et al., 2012; Silveira-Júnior et al., 2012; Takayama et al., 2012; Atoui et al., 2013; Castro et al., 2015; Simamoto-Júnior et al., 2015). Já as ligas de Co-Cr possuem uma combinação favorável de biocompatibilidade, uma resistência à corrosão, um favorável processo de fundição e, além disso, possui baixo custo (Rocha et al., 2006; Zupanic et al., 2006; Barbi et al., 2012; Kokolis et al., 2015). Portanto, os artigos apresentados nesta tese contemplam a utilização de ambas as ligas, sendo que ambas apresentaram resultados satisfatórios para este fator.

A configuração da junta é outro fator que influencia na resistência das juntas soldadas (Nunez-Pantoja et al., 2011; Nunez-Pantoja et al., 2012; Takayama et al., 2013, Simamoto Júnior et al., 2015, Kokolis et al., 2015). As juntas podem ser unidas por diferentes formatos. Alguns trabalhos mostraram que as juntas em formato da letra I, ou topo a topo, apresentam uma incompleta penetração tanto nas ligas de titânio (Castro et al., 2015; Simamoto Junior et al, 2015) quanto nas ligas de Co-Cr (Zupanic et al., 2006 e Kokolis et al., 2015), independentemente do tipo de técnica de soldagem utilizada. No trabalho de Simamoto Junior et al, (2015) a técnica de soldagem TIG associada a infraestruturas de Ti-6Al-4V com configuração da junta em X resultaram em juntas altamente resistentes com valores semelhantes ao grupo controle composto por infraestruturas intactas. Os artigos desta tese apresentaram

juntas em I e em X, entretanto não houve uma comparação direta dos tipos de junta. Por outro lado, observou-se que as junções em I apresentaram um grande vazio interno e as junções em X apresentaram vazios internos menores, semelhantes aos artigos supracitados.

Os métodos de avaliação das juntas soldadas se configuram como um fator muito importante no estudo dessas infraestruturas, tendo em vista o intuito de compreender seu comportamento mecânico e propor melhorias nas condições e técnicas de soldagem. Para tanto, muitos estudos têm utilizados testes não-destrutivos como inspeção radiográfica (Rocha et al., 2006; Nunez-Pantoja et al., 2011; Nunez-Pantoja et al., 2012; Simamoto-Júnior et al., 2015) associados a testes destrutivos tais como resistência à tração (Berg et al., 1995; Wang and Welsh, 1995; Chai and Chou, 1998; Taylor et al., 1998; Watanabe and Topham, 2006; Zupanic et al., 2006; Akman et al., 2008; Takayama et al., 2012; Atoui et al., 2013; Takayama et al., 2013; Castro et al., 2015), resistência à flexão (Rocha et al., 2006; Lyra e Silva et al., 2012; Atoui et al., 2013; Simamoto-Júnior et al., 2015) e dureza vicker's (Wang and Welsh, 1995; Takayama et al., 2012). Contudo, poucos estudos têm utilizado avaliação por micro-CT (Takayama et al., 2012; Takayama et al., 2013) e avaliação pelo método de elementos finitos (Castro et al., 2015). A avaliação por micro-CT permite avaliar tridimensionalmente e internamente toda a junta soldada, possibilitando não apenas identificar e calcular porosidades e vazios internos (Takayama et al., 2012; Takayama et al., 2013), mas também avaliar e calcular todo o volume de solda na junta. A avaliação pelo método de elementos finitos permite a construção de um modelo tridimensional aproximado ao que se tem experimentalmente e a análise das tensões nas diferentes regiões quando estes modelos são submetidos a cargas semelhantes ao que se tem nos ensaios experimentais (Castro et al., 2015). Os artigos apresentados utilizaram testes não destrutivos como inspeção radiográfica, líquidos penetrantes, micro-CT e método de elementos finitos associado a testes destrutivos de resistência à tração, dureza vicker's e resistência à flexão, o que permitiu um maior entendimento do comportamento mecânico dessas juntas.

No que concerne ao soldador, alguns autores (Takayama et al., 2012; Takayama et al., 2013) afirmam que diferentes soldadores bem como suas diferentes experiências também podem influenciar na qualidade da solda. Porém, nesses trabalhos, um único soldador experiente por vez soldou todas as amostras em um único momento, o que nos leva a cogitar que é possível que os efeitos dessa variável tenham sido minimizados nos trabalhos apresentados nesta tese.

Por fim, no que tange a afiação do eletrodo para as técnicas de soldagem TIG e Plasma, esta consiste em sempre manter o eletrodo de tungstênio não consumível afiado. Assim sendo, o mesmo necessita ser apontado de acordo com as especificações do fabricante do equipamento a cada novo ponto de solda para que, assim, possa se obter uma boa qualidade da junta soldada (Castro et al., 2015; Simamoto Júnior et al., 2015). Como esse requisito foi cumprido nos presentes trabalhos, é provável que esta variável não tenha exercido influencia nos resultados obtidos.

Por outro lado, é preciso o entendimento de como estes aparelhos funcionam clinicamente para que os valores encontrados laboratorialmente tenham validade clínica. Uma das maneiras de avaliar o aparelho estomatognático quanto ao desenvolvimento muscular e a função mastigatória é a FMM (Varga et al., 2011, Serra et al., 2013 Koc et al., 2010, Al-Omiri et al 2014), sendo que esta é influenciada por diversos fatores, dentre eles o tipo de tratamento reabilitador (Melo et al., 2016). Usuários de prótese totais convencionais apresentam eficiência mastigatória e FMM significativamente menores que pacientes totalmente dentados (Fontijn-Tekamp et al., 2000, Müller et al., 2001; Luraschi et al., 2011, Melo et al., 2016). Todavia, pacientes desdentados totais reabilitados com próteses sobre implantes apresentam uma melhoria significativa da estabilidade, retenção, função mastigatória e força muscular quando comparados com pacientes totalmente desdentados (Geckili et al., 2001; Kampen et al., 2005; Melo et al., 2016).

Assim sendo, estes estudos de FMM permitem a compreensão da força aplicada sobre estes aparelhos. Entretanto, pelo fato da mastigação ser composta por forças de diferentes naturezas, os valores e resultados obtidos

nos trabalhos laboratoriais não podem ser comparados diretamente com os resultados clínicos. Porém, este último artigo é o ponto de partida para que outros estudos clínicos sejam realizados para avaliação das infraestruturas propostas nos artigos laboratoriais.

## **5. Conclusões gerais**

- 1 – Ambas as técnicas de soldagem (laser e TIG ou Plasma) podem ser utilizadas para soldagem do Titânio;
- 2 – A técnica de soldagem TIG pode ser utilizada para soldagem do Co-Cr;
- 3 – Todas as amostras, independentemente da técnica utilizada, da configuração do equipamento, do tipo de liga e da configuração do equipamento, apresentaram vazios e porosidades internas em maior ou menor extensão;
- 4 – A variação do parâmetro duração do pulso não influenciou nos resultados obtidos;
- 5 – As juntas em formato da letra X apresentaram maior penetração da solda em relação às juntas em formato da letra I;
- 6 – Os métodos de avaliação não destrutivos exerceram importante papel no entendimento e compreensão do comportamento mecânico das infraestruturas;
- 6 – A experiência do soldador não influenciou os resultados obtidos, visto que o processo de soldagem foi executado por operadores únicos e calibrados;
- 7 – A afiação do eletrodo na técnica de soldagem TIG ou Plasma não influenciou os resultados obtidos, levando-se em consideração que todas as recomendações do fabricante foram atendidas;
- 8 – A reabilitação com implantes aumenta significativamente a FMM.

# **ANEXOS**